Two-electron transfer reactions in proteins: Bridge-mediated and proton-assisted processes

E. G. Petrov,[1] V. I. Teslenko,[1] and V. May[2]
[1]*Bogolyubov Institute for Theoretical Physics, Ukraine National Academy of Sciences, 14-b Metrologichna Street, UA-03143 Kiev, Ukraine*
[2]*Institut für Physik, Humboldt-Universität zu Berlin, Newtonstrasse 15, D-12489 Berlin, Germany*
(Received 4 June 2003; published 31 December 2003)

Nonadiabatic two-electron transfer (TET) reactions through donor-bridge-acceptor (DBA) systems is investigated within the approximation of fast vibrational relaxation. For TET reactions in which the population of bridging states remains small (less than 10^{-2}) it is demonstrated that a multiexponential transition process reduces to three-state kinetics. The transfer starts at the state with two excess electrons at the D center ($D^{2-}BA$), goes through the intermediate (transient) state with one electron at the D center and one at the A center ($D^{-}BA^{-}$), and ends up with the two electrons at the A center (DBA^{2-}). Furthermore, if the population of the intermediate state becomes also small the two-exponential kinetics can be transformed with high accuracy to single-exponential D-A TET kinetics. The related overall transfer rate contains contributions from stepwise and from concerted TET. The latter process is determined by a specific two-electron superexchange coupling incorporating the bridging states ($D^{-}B^{-}A$ and $DB^{-}A^{-}$) as well as the intermediate state ($D^{-}BA^{-}$). As an example, the reduction of micothione reductase by nicotinamide adenine dinucleotide phosphate is analyzed. Existing experimental data can be explained if one assumes that the proton-assisted reduction of the enzyme is realized by the concerted TET mechanism.

DOI: 10.1103/PhysRevE.68.061916 PACS number(s): 87.14.Ee, 34.30.+h, 82.20.Fd, 82.20.Rp

I. INTRODUCTION

Oxidation-reduction reactions which take place in biological systems are characterized by the transfer of electrons and protons through protein complexes, DNA fragments, or through the various phosphor lipid molecules of the cell membranes [1–8]. A number of these reactions refer to the multielectron type. The eight-electron reduction reaction of N_2 to ammonia in nitrogenase [9] and the four-electron reduction of O_2 to water in cytochrome *c* oxidase [10] are the most famous examples. Even the two-electron transfer (TET) reaction which represents the simplest multielectron transfer process proceeds in a much more complex way than the single-electron transfer. This difficulty has been clearly demonstrated for the two-electron cyclic voltametry in the model systems for flavoenzme activities [11] and for numerous chemical compounds [12–14]. Despite the fact that TET reactions in proteins are characterized by a number of intermediate electronic states related, for example, to the substrate-enzyme (S-E) complex, most of the oxidation-reduction reactions can be described by single- or two-exponential kinetics. We mention here the reaction in mycothione reductase [15], in monoohygenase [16], in nickel-iron hydrogenase [17], and in hemerythrin [18]. In noting that the observed single-exponential and two-exponential kinetics often result from underlying two-state or three-state systems, respectively, just such types of simple systems can be taken as reference models to describe TET processes. As an example, we refer to the three-state model used to describe donor-acceptor (D-A) TET in polar solution [19,20] (with an application of the Marcus theory of ET [21]).

In protein structures, numerous enzyme-catalyzed D-A TET reactions are accompanied by the uptake and/or the release of a single or a few protons. [For instance, the interconversion between vanadium (III) and oxovanadium (V) mediated by the vanadium haloperoxidases [22] proceeds as a proton-assisted TET process.] Of central importance for many catalyzed reactions is the hydride ($:H^{-}$) transfer, i.e., the transfer of the coupled system of two electrons and a single proton. Theoretical descriptions of hydride transfer are undertaken either by direct numerical simulations [23] or by the calculation of the transfer rate based on the Marcus theory of ET in D-A systems [24]. However, it might be also possible that proton-coupled TET occurs as a reducing equivalent, i.e., as a hydride fraction. Or alternatively, the proton and the electrons may be transferred stepwise [16].

Thus, there exists a real need for a suitable theory which is able to describe the various types of TET reactions including the single (two) proton-assisted TET. In contrast to this lack of a comprehensive TET theory, well-established models for single-electron transfer reactions exist [7]. Modified versions of this theory have been utilized to evaluate proton transfer reactions [25–28], proton-coupled ET [29,30], and hydrogen atom transfer [31,32]. But the question arises whether in such S-E complexes the sequential and/or the superexchange mechanism is responsible for the bridge-mediated D-A TET. (For example, it has been recently demonstrated that a two-electron reduction of flavin adenine dinucleotide (FAD) by quinone in fumarate reductase occurs along the chain of hemes or Fe-S clusters [33].) To characterize the importance of the sequential and the superexchange mechanisms for D-A TET reactions it seems to be most adequate to generalize the unified description of single-electron transfer as given in Refs. [34–42]. Therefore, we will follow our earlier approach (see Refs. [40–42]. Within this treatment of single-electron transfer, rate equations for the electronic state populations have been derived including nonadiabatic rate expressions which account for the superexchange as well as the sequential mechanism of ET.

It is the goal of the present paper to adopt this approach

and to develop a unified description of D-A TET capable of evaluating contributions from superexchange and sequential pathways through the bridging structure. For the special case of oxidation-reduction reactions where the TET proceeds against the background of fast protonation-deprotonation transitions in the electron-transferring molecular system, the given approach allows one to specify the *p*H dependence of nonadiabatic TET reactions in protein structures and to clarify the possible pathways of the TET reaction within the catalitic center of enzymes.

The paper is organized as follows. In Sec. II the derivation of the basic kinetic equations is presented. They incorporate concerted as well as stepwise pathways of nonadiabatic TET through the bridging structure. Furthermore, the respective rate constants and the overall transfer rates are quoted. To have an example or the distance dependence of the overall rate, D-A TET through a regular bridge is discussed in Sec. III. Additionally, the description of proton-assisted D-A TET valid for oxidation-reduction reactions accompanied by fast protonation-deprotonation transitions is given. An application of the theory to interpret experimental results on the TET reduction of mycothione reductase is presented in Sec. IV. In Sec. V, some general remarks on the interplay of concerted and stepwise mechanisms of D-A TET are presented.

II. KINETICS OF NONADIABATIC D-A TET PROCESSES

Distant TET will be considered in the following as a nonadiabatic reaction where the two electrons are transferred between spatially well separated D and A centers. In S-E complexes both centers are interconnected by specific molecular structures acting as a bridge. It is a characteristic feature of nonadiabatic ET that it proceeds against the background of considerably faster relaxation processes. Since we will study ET processes on a time scale much larger than the characteristic time τ_{rel} of the (intrastate) relaxation processes an essential simplification of the description becomes possible. As it is well established such a simplified description may be based on a coarse-grained approach [40–42]. In complex molecular structures such as proteins each electronic state is characterized by a number of different substates formed, e.g., by the associated or dissociated states of a S-E complex including protonated or deprotonated states of separate molecular groups. Here we will restrict ourself to such TET processes where the characteristic time τ_{subst} of the transitions between those substates which belong to the same electronic state largely exceeds τ_{rel} but remains much smaller than the characteristic time τ_{TET} of the TET reaction itself. The related inequality

$$\tau_{\mathrm{rel}} \ll \tau_{\mathrm{subst}} \ll \tau_{\mathrm{TET}} \tag{1}$$

represents the precondition to apply the coarse-grained description of transfer processes. But before utilizing this method we have to fix the model ready to describe TET reactions.

A. DBA model and basic rate equations

A comprehensive description of TET reaction in DBA systems has been given recently by us in Ref. [43]. Below, we will restrict to TET processes which take place via single-electron pathways. They are of most importance for short bridges where the Coulomb interaction between the transferred electrons substantially increases the energy gap between the initial donor (final acceptor) state and the intermediate bridging state. As a result the TET with the participation of single-electron bridge states becomes more effective compared to pathways where two electrons simultaneously occupy the bridge $\mathrm{B} \equiv (\mathrm{B}_1\mathrm{B}_2 \ldots \mathrm{B}_N)$ (see, i.e., the discussion in Ref. [44]). Single-electron pathways may dominate the TET reaction if the D and the A redox-centers are surrounded by polar groups while the bridge units B_m are exposed to a nonpolar medium (such a situation is typical for biosystems). In this case, polarization effects can essentially increase the energy gap $E(\mathrm{DB}^{2-}\mathrm{A}) - E(\mathrm{D}^{2-}\mathrm{BA})$ between the states related to a twofold occupied bridge and the reactant state. Roughly speaking, a restriction to single-electron pathways in the case of nonadiabatic TET becomes possible if the energy difference $E(\mathrm{DB}^{2-}\mathrm{A}) - E(\mathrm{D}^{-}\mathrm{B}^{-}\mathrm{A})$ exceeds 1 eV.

Let us introduce the set of electronic states of the DBA system involved in the TET reaction. The initial state of the TET reaction is given by the D center populated by two excess electrons:

$$|D\rangle \equiv |\mathrm{D}^{2-}\mathrm{B}_1\mathrm{B}_2 \cdots \mathrm{B}_m \cdots \mathrm{B}_N\mathrm{A}\rangle. \tag{2}$$

If one of the two electrons through the bridge we obtain the states

$$|B_m\rangle \equiv |\mathrm{D}^{-}\mathrm{B}_1\mathrm{B}_2 \cdots \mathrm{B}_m^{-} \cdots \mathrm{B}_N\mathrm{A}\rangle. \tag{3}$$

If the single electron arrived at the A center we get what will be considered in the following as the intermediate state of the TET process:

$$|I\rangle \equiv |\mathrm{D}^{-}\mathrm{B}_1\mathrm{B}_2 \cdots \mathrm{B}_m \cdots \mathrm{B}_N\mathrm{A}^{-}\rangle. \tag{4}$$

The state with one electron in the bridge B and one at the A center reads

$$|\tilde{B}_n\rangle = |\mathrm{DB}_1\mathrm{B}_2 \cdots \mathrm{B}_n^{-} \cdots \mathrm{B}_N\mathrm{A}^{-}\rangle, \tag{5}$$

and the product state of the reaction is given by

$$|A\rangle \equiv |\mathrm{DB}_1\mathrm{B}_2 \cdots \mathrm{B}_m \cdots \mathrm{B}_N\mathrm{A}^{2-}\rangle, \tag{6}$$

where both electrons arrived at the A center. (Here and below the electronic states and the sites of electron localization are denoted by capital italic and capital roman letters, respectively.) As already discussed, those states referring to a population of B with both electrons will not be taken into account. In this way we assume that the TET proceeds via the intermediate states $|I\rangle$ which are created after the first (single-electron) step of the TET.

The related electronic energies (minimum of the respective potential energy surfaces) are denoted by

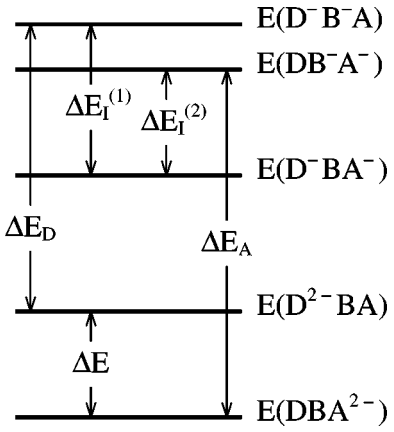

FIG. 1. Energetic position of the electronic states in the DBA system with a regular bridge.

$$E_D \equiv E(\mathrm{D}^{2-}\mathrm{BA}), \tag{7}$$

$$E_B \equiv E(\mathrm{D}^{-}\mathrm{B}^{-}\mathrm{A}), \tag{8}$$

$$E_I \equiv E(\mathrm{D}^{-}\mathrm{BA}^{-}), \tag{9}$$

$$E_{\tilde{B}} \equiv E(\mathrm{DB}^{-}\mathrm{A}^{-}), \tag{10}$$

and

$$E_A \equiv E(\mathrm{DBA}^{2-}). \tag{11}$$

For notational simplicity we had omitted the indices l_m specifying the conformational states of the DBA system. Moreover, Eqs. (8) and (10) assume that the two categories of the N states with a single electron in the bridge [the states $|B_m\rangle$, Eq. (3), and the states $|\tilde{B}_n\rangle$, Eq. (5)], are each characterized by the set of energies $E(\mathrm{D}^{-}\mathrm{B}_1^{-}B_2\cdots\mathrm{B}_m\cdots\mathrm{B}_N\mathrm{A}) \approx E(\mathrm{D}^{-}\mathrm{B}_1\mathrm{B}_2\cdots\mathrm{B}_m^{-}\cdots\mathrm{B}_N\mathrm{A}) \approx E(\mathrm{D}^{-}\mathrm{B}_1\mathrm{B}_2\cdots\mathrm{B}_m\cdots\mathrm{B}_N^{-}\mathrm{A}) \equiv E(\mathrm{D}^{-}\mathrm{B}^{-}\mathrm{A}) \equiv E_B$ and $E(\mathrm{DB}_1^{-}\mathrm{B}_2\cdots\mathrm{B}_m\cdots\mathrm{B}_N\mathrm{A}^{-}) \approx E(\mathrm{DB}_1\mathrm{B}_2\cdots\mathrm{B}_m^{-}\cdots\mathrm{B}_N\mathrm{A}^{-}) \approx E(\mathrm{DB}_1\mathrm{B}_2\cdots\mathrm{B}_m\cdots\mathrm{B}_N^{-}\mathrm{A}^{-}) \equiv E(\mathrm{DB}^{-}\mathrm{A}^{-}) \equiv E_{\tilde{B}}$, respectively. The relative positions of these energies are shown in Fig. 1. To have a positive driving force for the overall TET reaction E_A has to be positioned at the bottom of the energy scheme. Although two excess electrons are located at the A part of the DBA system a huge reorganization stabilizes this state against all other states. A similar assumption of a remarkable reorganization has been taken for the initial state of the TET. Because of that reorganization E_D could be placed just above E_A. If we provide that a possible energy reorganization of the bridge B upon the presence of a single excess electron at any mth unit is less than that of the D and the A, the arrangement of the remaining levels shown in Fig. 1 becomes clear, i.e., E_B and $E_{\tilde{B}}$ have been positioned at the top and E_I in between. The sequence of E_B and $E_{\tilde{B}}$, however, seems to be somewhat arbitrary but setting $E_{\tilde{B}} > E_B$ may correspond to the fact that the A shows the biggest reorganization if excess electrons are present.

To achieve a unified description of nonadiabatic electron-transfer processes as in the case of single-electron transfer

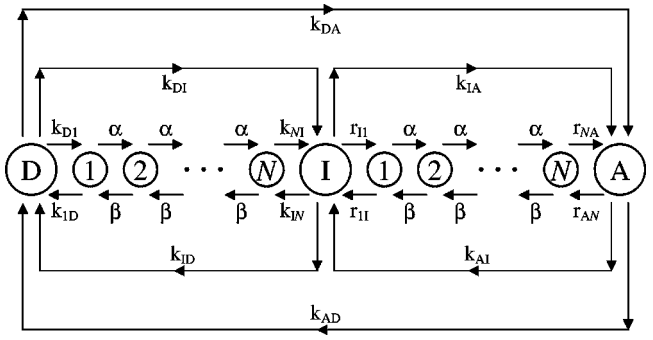

FIG. 2. Kinetic scheme of the D-A TET process through a regular bridge of N units.

the TET Hamiltonian is written in local electron-vibrational states $|M\{v_M\}\rangle$ (note the introduction of the symbol M which additionally accounts for the presence of electronic sublevels denoted by l). Its diagonal part reads

$$H_0 = \sum_M \sum_{\{v_M\}} E(M\{v_M\})|M\{v_M\}\rangle\langle M\{v_M\}|, \tag{12}$$

whereas the off-diagonal part is given by

$$V = \sum_{M,M'} \sum_{\{v_M\}\{v'_{M'}\}} V_{M\{v_M\}M'\{v'_{M'}\}}|M\{v_M\}\rangle\langle M'\{v_{M'}\}|. \tag{13}$$

$E(M\{v_M\})$ are the two-electron vibrational energies of the DBA system, for example, if $M = Dl_D$ then $E(Dl_D, \{v_{l_D}\})$ is the energy of the $\{v_{l_D}\}$th vibrational level of the l_Dth substate belonging to the electronic state with both electrons located at the D. Furthermore, to give another example, if $M = \tilde{B}_n l_{\tilde{B}n}$ then $E(\tilde{B}_n, l_{\tilde{B}_n}\{v_{\tilde{B}_n}\})$ is the energy of the $\{v_{\tilde{B}_n}\}$th vibrational level of the $l_{\tilde{B}_n}$th substate belonging the $\tilde{B}_n$th electronic state. The coupling among all these types of states is described by $V_{M\{v_M\}M'\{v_{M'}\}}$. It accounts for electron-vibrational transitions between different substates l_m and l'_m of the same electronic state m ($M = ml_m$, $M' = ml'_m$), or between the substates l_m and $l_{m'}$ belonging the different electronic states m and m' ($M = ml_m, M' = m'l_{m'}$).

The introduced TET model is of such a type that we can directly use the technique of Refs. [40–42] to derive a set of coarse-grained rate equations for the populations of all states introduced so far. (A short explanation of how to derive the rate equations can be found in Appendix A.) The populations for which time evolution is described by the rate equations are $P_D(t)$, $P_I(t)$, and $P_A(t)$ for the basic electronic states, Eqs. (2), (4), and (6). Moreover, we have to consider the populations $P_m(t)$ and $\tilde{P}_n(t)$ referring to the first and the second type of bridging states, Eqs. (3) and (5), respectively. According to the notation of all rate constants as given in scheme of Fig. 2 the set of equations for the state populations reads

$$\dot{P}_D(t) = -(q_D + k_{DA})P_D(t) + k_{1D}P_1(t) + k_{ID}P_I(t) + k_{AD}P_A(t), \tag{14}$$

$$\dot{P}_1(t) = -q_1 P_1(t) + k_{D1}P_D(t) + \beta P_2(t), \tag{15}$$

$$\dot{P}_m(t) = -qP_m(t) + \alpha P_{m-1}(t) + \beta P_{m+1}(t), \quad (m = 2,3,\ldots,N-1), \tag{16}$$

$$\dot{P}_N(t) = -q_N P_N(t) + k_{IN}P_I(t) + \alpha P_{N-1}(t), \tag{17}$$

$$\dot{P}_I(t) = -(q_I^{(1)} + q_I^{(2)})P_I(t) + k_{NI}P_N(t) + k_{DI}P_D(t) + r_{1I}\tilde{P}_1(t) + k_{AI}P_A(t), \tag{18}$$

$$\dot{\tilde{P}}_1(t) = -\tilde{q}_1\tilde{P}_1(t) + r_{I1}P_I(t) + \beta\tilde{P}_2(t), \tag{19}$$

$$\dot{\tilde{P}}_n(t) = -q\tilde{P}_n(t) + \alpha\tilde{P}_{n-1}(t) + \beta\tilde{P}_{n+1}(t), \quad (n = 2,3,\ldots,N-1), \tag{20}$$

$$\dot{\tilde{P}}_N(t) = -\tilde{q}_N\tilde{P}_N(t) + r_{AN}P_A(t) + \alpha\tilde{P}_{N-1}(t), \tag{21}$$

$$\dot{P}_A(t) = -(q_A + k_{AD})P_A(t) + r_{NA}\tilde{P}_N(t) + k_{IA}P_I(t) + k_{DA}P_D(t). \tag{22}$$

These rate equations have to be complemented by the following abbreviations introduced for different rate expressions

$$q_D \equiv k_{D1} + k_{DI}, \quad q_1 \equiv k_{1D} + \alpha, \quad q_N \equiv k_{NI} + \beta,$$

$$\tilde{q}_1 \equiv r_{1I} + \alpha, \quad \tilde{q}_N \equiv r_{NA} + \beta,$$

$$q_A \equiv r_{AN} + k_{AI}, \quad q_I^{(1)} \equiv k_{IN} + k_{ID}, \quad q_I^{(2)} \equiv r_{I1} + k_{IA},$$

$$q \equiv \alpha + \beta. \tag{23}$$

For the numerical calculations presented later we have used rate expressions of the Marcus form,

$$k_{mn} = \frac{2\pi}{\hbar}\frac{|V_{nm}|^2}{\sqrt{4\pi\lambda_{mn}k_BT}}\exp\left[-\frac{(\Delta E_{mn} - \lambda_{mn})^2}{4\lambda_{mn}k_BT}\right], \tag{24}$$

which are widely employed for the description of distant D-A ET in biological systems [2,3,5–8]. If the rates belong to superexchange transitions the coupling matrices V_{mn} are effective quantities formed by the elementary transfer integrals which couple neighboring sites (cf. Appendix B). For the other cases V_{mn} are given by the elementary transfer integrals. The various energy gaps ΔE_{mn} in Eq. (24) are defined as follows (see also Fig. 1). Those participating in the first single-electron transfer step are

$$\Delta E_{1D} \equiv \Delta E_D = E(\mathrm{D^-B^-A}) - E(\mathrm{D^{2-}BA}),$$

$$\Delta E_{NI} \equiv \Delta E_I^{(1)} = E(\mathrm{D^-B^-A}) - E(\mathrm{D^-BA^-}),$$

and

$$\Delta E_{ID} = E(\mathrm{D^-BA^-}) - E(\mathrm{D^{2-}BA}) = \Delta E_D - \Delta E_I^{(1)}.$$

The corresponding reorganization energies λ_{mn} are denoted as λ_{1D}, λ_{NI}, and λ_{ID}. r_{mn} describing the second step of the TET reaction have the same form as in Eq. (24), but the transfer coupling matrix elements V_{D1}, V_{AN}, and V_{ID} have to be replaced by V'_{D1}, V'_{AN}, and V_{AI}, respectively. Furthermore, the energy gaps and the corresponding reorganization energies are

$$\Delta E_{1I} \equiv \Delta E_I^{(2)} = E(\mathrm{DB^-A^-}) - E(\mathrm{D^-BA^-}),$$

$$\Delta E_{NA} \equiv \Delta E_A = E(\mathrm{DB^-A^-}) - E(\mathrm{DBA^{2-}}),$$

$$\Delta E_{IA} = E(\mathrm{D^-BA^-}) - E(\mathrm{DBA^{2-}}) = \Delta E_A - \Delta E_I^{(2)},$$

and

$$\lambda_{1I},\ \lambda_{NA},\ \lambda_{IA},$$

respectively. In the case of the two-electron superexchange rate constant k_{DA} (k_{AD}) we take $\Delta E_{DA} \equiv \Delta E = E(\mathrm{D^{2-}BA}) - E(\mathrm{DBA^{2-}})$ and the reorganization energy λ_{DA}. The rate of the sequential electron motion along the regular B are taken as

$$\alpha = \beta = \frac{2\pi}{\hbar}\frac{|V_B|^2}{\sqrt{4\pi\lambda_B k_B T}}\exp\left[-\frac{\lambda_B}{4\lambda_B k_B T}\right], \tag{25}$$

where it has been assumed that the bridge driving forces vanish. $|V_B| \equiv |V_{mm+1}| = |V_{mm-1}|$ and λ_B denote the electronic coupling and the reorganization energy, respectively.

B. Reduced set of kinetic equations

The TET reaction described by the rate equations (14)–(22) is determined by a multiexponential law with $2(N+1)$ different transfer rates $K_1, K_2, \ldots, K_{2N+2}$ In the most general case it is only possible to determine the rates by numerical methods. However, in the regime of the so-called D-A TET, analytical expressions for the overall rates can be derived and a detailed analysis of the TET reaction becomes possible. The D-A TET regime is met if the integral population of the bridging structure, $P_B(t)$, remains very small during the transfer. To derive reduced rate equations valid for this D-A TET regime we follow our approach given in Ref. [42]. To start with we define the integral bridge population as

$$P_B(t) = \sum_{m=1}^{N} P_m(t) + \sum_{n=1}^{N} \tilde{P}_n(t) \ll 1. \tag{26}$$

It is our aim to reduce the large set of rate equations (22) to a set of three equations valid for the population of the basic states, Eqs. (2), (4), and (6). It follows (for details see Refs. [42,43]) that

$$\dot{P}_D(t) = -(k_f^{(1)} + k_{DA})P_D(t) + k_b^{(1)}P_I(t) + k_{AD}P_A(t),$$

$$\dot{P}_I(t) = -(k_f^{(2)} + k_b^{(1)})P_I(t) + k_f^{(1)}P_D(t) + k_b^{(2)}P_A(t),$$

$$\dot{P}_A(t) = -(k_b^{(2)} + k_{AD})P_A(t) + k_f^{(2)}P_I(t) + k_{DA}P_D(t). \tag{27}$$

The effective forward (f) and effective backward (b) rates are given by a specific combination of those rate constants appearing in the initially derived rate equations (14)–(22):

$$k_f^{(1)} = k_{DI} + k_{DI}^{(seq)}, \quad k_b^{(1)} = k_{ID} + k_{ID}^{(seq)},$$

$$k_{DI}^{(seq)} = k_{D1}k_{NI}\alpha^{N-1}/D_1, \quad k_{ID}^{(seq)} = k_{1D}k_{IN}\beta^{N-1}/D_1, \tag{28}$$

and

$$k_f^{(2)} = k_{IA} + k_{IA}^{(seq)}, \quad k_b^{(2)} = k_{AI} + k_{AI}^{(seq)},$$

$$k_{IA}^{(seq)} = r_{I1}r_{NA}\alpha^{N-1}/D_2, \quad k_{AI}^{(seq)} = r_{1I}r_{AN}\beta^{N-1}/D_2, \tag{29}$$

where

$$D_1 = k_{NI}\alpha^{N-1} + k_{1D}\beta^{N-1} + k_{1D}k_{NI}D(N-2),$$

$$D_2 = r_{NA}\alpha^{N-1} + r_{1I}\beta^{N-1} + r_{1I}r_{NA}D(N-2), \tag{30}$$

and

$$D(M) = (\alpha\beta)^{M/2}\frac{\sinh[\chi(M+1)]}{\sinh\chi}, \quad [e^{\chi} = (\alpha/\beta)^{1/2}]. \tag{31}$$

The rate expressions (28) characterize the forward transitions related to the first and the second single-electron step of the common TET process and the rate expressions (29) are valid for the backward transitions. Each transfer rate includes superexchange contributions (rates k_{DI}, k_{ID} and k_{IA}, k_{AI}) and sequential contributions (rates $k_{DI}^{(seq)}$, $k_{ID}^{(seq)}$ and $k_{IA}^{(seq)}$, $k_{AI}^{(seq)}$) pointing out the complex character of both single-electron steps of the TET reaction.

Note that the TET process is also defined by the direct pathways, $(D^{2-} + A \rightarrow D + A^{2-})$ and $(D^{2-} + A \leftarrow D + A^{2-})$. The corresponding transfer rates k_{DA} and k_{AD} are caused by the repeated superexchange between D and A centers (see Appendix B). Just this type of superexchange leads to the concerted mechanism of the TET reaction along a single bridge.

The *exact* solution of Eqs. (27) is simply obtained as

$$P_J(t) = P_J(\infty) + C_J^{(1)}e^{-K_1 t} + C_J^{(2)}e^{-K_2 t}, \quad (J = D, I, A), \tag{32}$$

where

$$P_D(\infty) = (a_1 k_b^{(1)} + d_2 k_f^{(2)})/(a_1 d_1 - a_2 d_2),$$

$$P_A(\infty) = (a_2 k_b^{(1)} + d_1 k_f^{(2)})/(a_1 d_1 - a_2 d_2),$$

$$P_I(\infty) = 1 - P_D(\infty) - P_A(\infty) \tag{33}$$

are the steady state populations of the respective states. The concrete form of $C_J^{(1)}$ and $C_J^{(2)}$ follows from the normalization condition $P_D(t) + P_I(t) + P_A(t) \approx 1$ and the initial condition which is taken here as $P_D(0) = 1$, $P_I(0) = 0$, $P_A(0) = 0$, $P_B(0) = 0$. One obtains

$$C_D^{(1)} = \frac{K_1 + P_D(\infty)K_2 - a_1 - k_b^{(1)}}{K_1 - K_2},$$

$$C_D^{(2)} = \frac{a_1 + k_b^{(1)} - K_2 - P_D(\infty)K_1}{K_1 - K_2},$$

$$C_A^{(1)} = \frac{P_A(\infty)K_2 - a_2 - k_f^{(2)}}{K_1 - K_2}, \quad C_A^{(2)} = \frac{a_2 + k_f^{(2)} - P_A(\infty)K_1}{K_1 - K_2},$$

$$C_I^{(1)} = -(C_D^{(1)} + C_A^{(1)}), \quad C_I^{(2)} = -(C_D^{(2)} + C_A^{(2)}). \tag{34}$$

The overall transfer rates read

$$K_1 = \tfrac{1}{2}[a_1 + d_1 + \sqrt{(a_1 - d_1)^2 + 4a_2 d_2}],$$

$$K_2 = \tfrac{1}{2}[a_1 + d_1 - \sqrt{(a_1 - d_1)^2 + 4a_2 d_2}], \tag{35}$$

where

$$a_1 \equiv k_f^{(2)} + k_b^{(2)} + k_{AD}, \quad a_2 \equiv k_{DA} - k_f^{(2)},$$

$$d_1 \equiv k_f^{(1)} + k_b^{(1)} + k_{DA}, \quad d_2 \equiv k_{AD} - k_b^{(1)}. \tag{36}$$

Figure 3 shows the excellent agreement between the description of the D-A TET kinetics by an exact numerical solution of the set of Eqs. (22) and by the approximate analytical solution (coarse-grained approach), Eq. (32). The analysis shows that such an agreement persists if the bridge population P_B does not exceed 10^{-2}. Note that the bridge populations $P_m(t)$ and $\tilde{P}_n(t)$ exhibit a multiexponential time behavior with fast and slow kinetic phases, Fig. 3(b), although the state populations $P_D(t)$, $P_I(t)$, and $P_A(t)$ follow a two-exponential evolution. But, due to the inequality (26) the fast kinetic phases do not influence the time dependence of the $|D\rangle$, $|I\rangle$, and $|A\rangle$ state populations.

III. SINGLE-EXPONENTIAL D-A TET

Let us suppose that the population of the intermediate electronic state $|I\rangle$, Eq. (4), becomes small during the D-A TET. Therefore the condition (26) has to be complemented by the inequality

$$P_I(t) \ll 1. \tag{37}$$

The inspection of the coarse-grained solution shows that this inequality is satisfied if

$$k_b^{(1)}, k_f^{(2)} \gg k_f^{(1)}, k_b^{(2)}, \tag{38}$$

what finally results in the relation $K_1 \gg K_2$. Concentrating on the time scale $\Delta t \gg K_1^{-1}$ single-exponential kinetics is obtained:

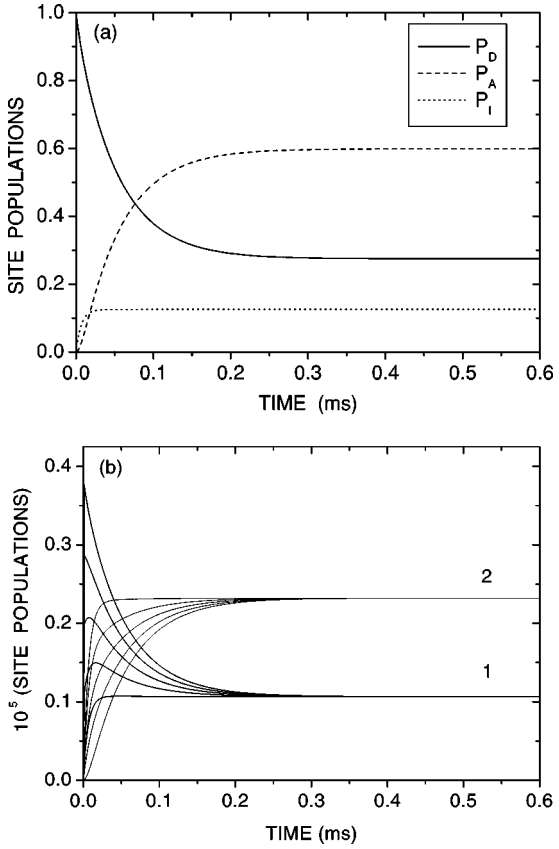

FIG. 3. Kinetics of the D-A TET process described by the exact numerical solution of Eqs. (22) and the analytic two-exponential solution (32). The two-exponential evolution of the donor, acceptor and intermediate state population completely coincides with the exact evolution [panel (a)] despite the fact that the bridge state populations exhibit a multiexponential time behavior [panel (b)]. The rate constants (24) are taken at $\Delta E_D=\Delta E_A=0.32$ eV, $\Delta E_I^{(1)}=0.30$ eV, $\Delta E_I^{(2)}=0.28$ eV; $\lambda_{1D}=\lambda_{NI}=\lambda_{ID}=0.8$ eV, $\lambda_{1I}=\lambda_{NA}=\lambda_{IA}=0.5$ eV, $\lambda_{DA}=1$ eV, $\lambda_B=0.7$ eV; $V_{D1}=V_{NA}=V'_{D1}=V'_{NA}=0.02$ eV, $V_B=0.03$ eV, $V_{D1}=0.02$ eV; $N=5$, $T=298$ K. The notations 1 and 2 [panel (b)] indicate the set of curves $P_m=P_m(t)$, $(m=1,2,\ldots,5)$ and $\tilde{P}_n=\tilde{P}_n(t)$, $(n=1,2,\ldots,5)$ for bridge populations which appear at the first and the second single-electron stage of the common TET process, respectively. [Note that bridge populations are smaller by the factor 10^{-5} than the intermediate state populations P_I shown in panel (a).]

$$P_D(t)\simeq P_D(\infty)+[1-P_D(\infty)]e^{-K_{\mathrm{TET}}t},$$

$$P_A(t)\simeq P_A(\infty)(1-e^{-K_{\mathrm{TET}}t}). \tag{39}$$

The overall D-A TET rate $K_{\mathrm{TET}}=K_2$ takes the form

$$K_{\mathrm{TET}}=\tau_{\mathrm{TET}}^{-1}=K_{\mathrm{TET}}^{(\mathrm{step})}+K_{\mathrm{TET}}^{(\mathrm{conc})}. \tag{40}$$

The rates $K_{\mathrm{TET}}^{(\mathrm{step})}$ and $K_{\mathrm{TET}}^{(\mathrm{conc})}$ are originated by the stepwise and of the concerted mechanism, respectively. Both are represented as a sum of corresponding forward and backward transfer rates so that we get

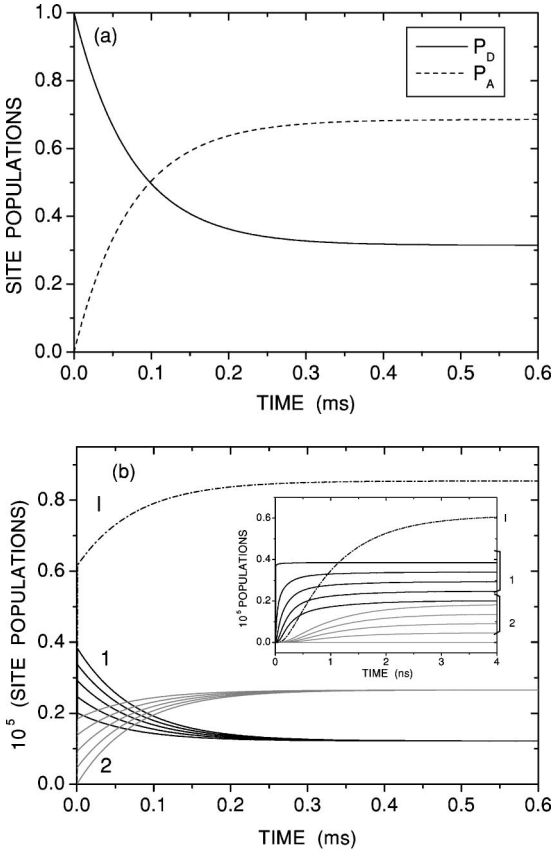

FIG. 4. Kinetics of the D-A TET process decribed by the exact numerical solution of Eqs. (22) and the analytic two-exponential solution (39). The two-exponential evolution of the donor and the acceptor population completely coincides with the exact evolution [panel (a)] despite the fact that the intermediate and bridge state populations exhibit a multiexponential time evolution [panel (b)]. The index I indicates the curve $P_I=P_I(t)$. For the notation 1 and 2 [panel (b) including the insert] see Fig. 3. Equations (24) are calculated for the same parameters as in Fig. 3 except $\Delta E_I^{(1)}=0.005$ eV and $\Delta E_I^{(2)}=0.003$ eV.

$$K_{\mathrm{TET}}^{(\mathrm{step})}=K_{\mathrm{step}}^{(\mathrm{f})}+K_{\mathrm{step}}^{(\mathrm{b})},\quad K_{\mathrm{step}}^{(\mathrm{f})}=\frac{k_{DI}k_{IA}}{k_{ID}+k_{IA}},\quad K_{\mathrm{step}}^{(\mathrm{b})}=\frac{k_{AI}k_{ID}}{k_{ID}+k_{IA}}, \tag{41}$$

and

$$K_{\mathrm{TET}}^{(\mathrm{conc})}=K_{\mathrm{conc}}^{(\mathrm{f})}+K_{\mathrm{conc}}^{(\mathrm{b})},\quad K_{\mathrm{conc}}^{(\mathrm{f})}=k_{DA},\quad K_{\mathrm{conc}}^{(\mathrm{b})}=k_{AD}. \tag{42}$$

Figure 4 confirms the validity of the single-exponential description of the bridge-mediated D-A TET reaction based on Eqs. (39)–(42). (A single-exponential description is valid if $P_B, P_I<10^{-2}$.) Although the evolution of the bridge and intermediate state populations includes fast components, as shown in Fig. 4(b), the fast kinetic phases does not influence the evolution of the donor and the acceptor populations, what is justified by Fig. 4(a). In what follows we will consider two example for a single-exponential description of bridge-mediated D-A TET processes.

A. Length dependence of D-A TET overall transfer rate

A dependence of the overall D-A TET rate on the number of bridge units N can be found in the stepwise as well as the concerted contribution. Let us introduce the sequential decay parameter

$$\xi_1=\frac{k_{1D}[k_{NI}-\alpha(1-\gamma)]}{\alpha(k_{NI}+k_{1D})}. \tag{43}$$

It characterizes the electron hopping in the course of the first single-electron bridge-mediated pathway. That for the second single-electron bridge-mediated pathway reads

$$\xi_2=\frac{r_{1I}[r_{NA}-\alpha(1-\gamma)]}{\alpha(k_{NA}+k_{1I})}. \tag{44}$$

Respective superexchange decay parameters can be introduced as

$$\zeta_1=-2\ln\left[\frac{|V_B|}{(\Delta E_D\Delta E_I^{(1)})^{1/2}}\right], \tag{45}$$

and

$$\zeta_2=-2\ln\left[\frac{|V_B|}{(\Delta E_A\Delta E_I^{(2)})^{1/2}}\right]. \tag{46}$$

Then, the transfer rates related to the stepwise pathway, Eqs. (28) and (29), can be written in the following form:

$$k_{DI}=k_{DI}^{(0sup)}e^{-\zeta_1(N-1)}+\frac{k_{DI}^{(0seq)}}{1+\xi_1R(N)},$$

$$k_{ID}=k_{ID}^{(0sup)}e^{-\zeta_1(N-1)}+\frac{k_{ID}^{(0seq)}[1-(1-\gamma)R(N)]}{1+\xi_1R(N)},$$

$$k_{IA}=k_{IA}^{(0sup)}e^{-\zeta_2(N-1)}+\frac{k_{IA}^{(0seq)}}{1+\xi_2R(N)},$$

$$k_{AI}=k_{AI}^{(0sup)}e^{-\zeta_2(N-1)}+\frac{k_{AI}^{(0seq)}[1-(1-\gamma)R(N)]}{1+\xi_2R(N)}. \tag{47}$$

In Eqs. (45) and (46) the quantities $\Delta E_{ID}=\Delta E_D-\Delta E_I^{(1)}$, and $\Delta E_{IA}=\Delta E_A-\Delta E_I^{(2)}$ are the gaps between the energy position of intermediate state $|I\rangle$ and the $|D\rangle$ and $|A\rangle$ state, respectively (see Fig. 1). Note, that the N-dependence of the sequential mechanism of single-electron transfer is contained in the factor

$$R(N)=\frac{1-\gamma^{N-1}}{1-\gamma}, \quad (\gamma\equiv\beta/\alpha\leqslant 1). \tag{48}$$

The quantities

$$k_{DI}^{(0seq)}=\frac{k_{D1}k_{NI}}{k_{NI}+k_{1D}}, \quad k_{ID}^{(0seq)}=\frac{k_{IN}k_{1D}}{k_{NI}+k_{1D}},$$

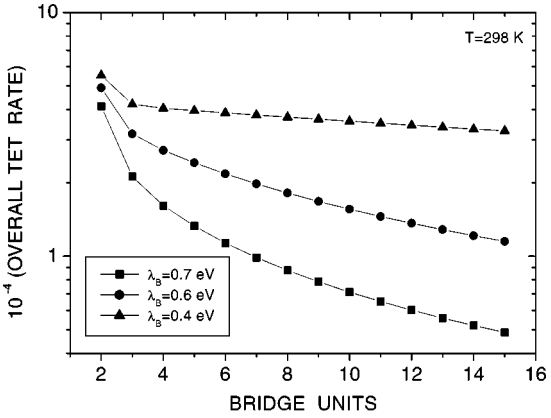

FIG. 5. Distance dependence of the D-A TET overall transfer rate (40) obtained from Eqs. (47) and (53). The calculation of the rate constants are performed with parameters identical to those of Fig. 4 except $\lambda_B=0.4,0.6,0.7$ eV. The superexchange mechanism dominates at $N=2,3$ while at $N>3$ the main contribution to the rate stems from the sequential mechanism. At the given parameters, both mechanisms form a stepwise pathway of D-A TET.

$$k_{IA}^{(0seq)}=\frac{r_{I1}r_{NA}}{r_{NA}+k_{1I}}, \quad k_{AI}^{(0seq)}=\frac{r_{AN}r_{1I}}{r_{NA}+r_{1I}}, \tag{49}$$

and

$$k_{DI(ID)}^{(0sup)}=\frac{2\pi}{\hbar}\frac{|V_{D1}V_{NA}|^2}{\Delta E_D\Delta E_I^{(1)}}(FC)_{D\to I(I\to D)},$$

$$k_{IA(AI)}^{(0sup)}=\frac{2\pi}{\hbar}\frac{|V'_{D1}V'_{NA}|^2}{\Delta E_A\Delta E_I^{(2)}}(FC)_{I\to A(A\to I)} \tag{50}$$

are rates of sequential and superexchange transfer through a bridge with a single unit, respectively.

Introducing the two-electron superexchange decay parameters

$$\zeta'_1=-2\ln\left[\frac{|V_B|}{(\Delta E_D\Delta\tilde{E}_D)^{1/2}}\right], \quad (\tilde{E}_D=\Delta E_D+\Delta E_I^{(2)}-\Delta E_I^{(1)}), \tag{51}$$

and

$$\zeta'_2=-2\ln\left[\frac{|V_B|}{(\Delta E_A\Delta\tilde{E}_A)^{1/2}}\right], \quad (\tilde{E}_A=\Delta E_A+\Delta E_I^{(1)}-\Delta E_I^{(2)}) \tag{52}$$

the respective rates can be written as

$$k_{DA(AD)}=k_{DA(AD)}^{(0)}e^{-\zeta(N-1)}, \quad (\zeta=\zeta'_1+\zeta'_2), \tag{53}$$

where $k_{DA(AD)}^{(0)}$ is the two-electron superexchange transfer rate through a bridge with a single unit.

Equations (28) and (29) together with the concrete expressions for the transfer rates, Eqs. (47) and (53), allow us to estimate the length dependence of the D-A TET for different transfer regimes. As an example, we will consider this length

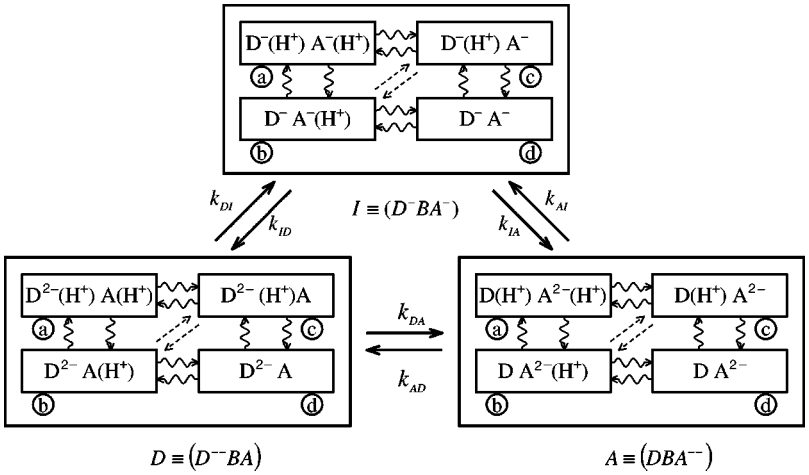

FIG. 6. Kinetic scheme of the D-A TET in a model where the transient state *I*, Eq. (4), corresponds to a singly oxidated donor and singly reduced acceptor center. *a* and *d* denote the electronic substates with two accepted and two released protons, respectively, wheras *b* and *c* give the substates with one accepted and one released proton. Wavy lines indicate the fast single-particle protonation/deprotonation process; the proton exchange between the D and A centers is represented by the dashed arrows. (Since the energies of bridge units are assumed to be independent of the *p*H value the symbols $B_1, \ldots, B_N$ are omitted in scheme).

dependence for different hopping rates $\alpha(=\beta)$. The different values of α follow from a variation of the related reorganization energy λ_B. According to Eqs. (43) and (44) for the sequential decay parameters and Eqs. (45) and (46) for the superexchange decay parameters both types of parameters decrease for an increasing λ_B (due to the increase of α). Figure 5 displays the N dependence of K_{TET} at the stepwise regime of TET, where $K_{\mathrm{TET}} \approx K_{\mathrm{TET}}^{(\mathrm{step})}$ [see Eq. (40)]. Although the concerted contribution remains small for the given set of parameters the superexchange (single-electron) mechanism dominates at a short bridge with $N=2,3$. When the number of bridge units exceeds three, the main contribution to K_{TET} stems from the sequential D-A TET mechanism. Just originated by this contribution K_{TET} shows a much weaker decrease when the reorganization energy λ_B decreases (compare the values $\xi_1=0.40$, $\xi_2=6.33$ at $\lambda_B=0.7$ eV and the values $\xi_1=0.016$, $\xi_2=0.26$ at $\lambda_B=0.4$ eV).

B. *p*H dependence of the D-A TET overall transfer rate

It has been shown in the preceding section that the D-A TET can be reduced to the transitions between three electronic states $|D\rangle$, $|I\rangle$, and $|A\rangle$ if the bridge population remains small. In biosystems, as a rule, each electronic state has to be charcaterized by a manifold of substates. Accordingly, the D-A TET reactions have to be analyzed by taking into account all these substates. In the following, we will consider D-A TET in such systems where the substates are only associated with protonated and deprotonated groups of the donor and the acceptor, while each bridge unit is defined by a single electronic term only. It means that each electronic state $|m\rangle = |D\rangle, |I\rangle, |A\rangle$ is characterized by its protonated ($l_m=\mathrm{p}$) and deprotonated ($l_m=\mathrm{dp}$) substate (see Appendix A). The protonation-deprotonation processes are supposed to be fast enough so that the D-A TET rate constants k_{mn} can be defined by Eq. (A9). In this expression the contributions from the various protonated-deprotonated ET channels are defined by the substate weights $Q_{l_m}^{(m)}$, Eq. (A6), and by the substate-substate rate constants $k_{ml_m \to nl_n}$, Eq. (A2). To specify $Q_{l_m}^{(m)}$ we restrict ourself to the case where the protonation or deprotonation of the D and the A centers proceed independently. Therefore we may write

$$Q_a^{(m)} = f_{\mathrm{p\,D}}^{(m)} f_{\mathrm{p\,A}}^{(m)}, \quad Q_b^{(m)} = f_{\mathrm{dp\,D}}^{(m)} f_{\mathrm{p\,A}}^{(m)}$$

$$Q_c^{(m)} = f_{\mathrm{p\,D}}^{(m)} f_{\mathrm{dp\,A}}^{(m)}, \quad Q_d^{(m)} = f_{\mathrm{dp\,D}}^{(m)} f_{\mathrm{dp\,A}}^{(m)}, \tag{54}$$

where the statistical weights have been introduced for the protonated ($f_{\mathrm{p\,D}}^{(m)}$, $f_{\mathrm{p\,A}}^{(m)}$) and the deprotonated ($f_{\mathrm{dp\,D}}^{(m)}$, $f_{\mathrm{dp\,A}}^{(m)}$) centers D and A and for the case where the DBA system is in its mth electronic state. The standard expression for the weights reads

$$f_{\mathrm{p}}^{(m\mathrm{L})} = \frac{[\mathrm{H}^+]}{[\mathrm{H}^+] + K_L^{(m)}}, \quad f_{\mathrm{dp}}^{(m\mathrm{L})} = \frac{K_L^{(m)}}{[\mathrm{H}^+] + K_L^{(m)}}, \tag{55}$$

where $[\mathrm{H}^+]$ is the proton concentration and $K_L^{(m)}$ is the dissociation constant for the $L=\mathrm{D}$ and $L=\mathrm{A}$ centers The scheme of substates belonging each to a separate electronic state is depicted in Fig. 6. Every electronic state includes a manifold of four protonated and deprotonated substates denoted by *a*, *b*, *c*, and *d*. The large boxes refer to the initial (D), the transient (I), and the final (A) electronic states which include all the mentioned substates shown in the small boxes.

The kinetic processes shown in Fig. 6 are described by a set of three coupled equations like those of Eq. (27). The time evolution of the state populations, $P_D(t)$, $P_I(t)$, and $P_A(t)$, is given by Eq. (32). Here we consider the single-exponential limit, Eq. (39), which is valid for $P_I(t) \ll 1$ [cf. Eq. (37)]. For a small population of the transient/intermediate electronic state *I*, the kinetics is characterized by an overall D-A ET transfer rate K_{TET}, Eq. (40). The concerted and stepwise contribution to the overall D-A TET can be estimated in comparing the transfer rates $K_{\mathrm{conc}}^{(\mathrm{f})}$ and $K_{\mathrm{step}}^{(\mathrm{f})}$. The concerted TET is defined as a process for which two electrons change their location in a single hop without alteration of the proton location. It means that the corresponding partial rate constants obey the property $k_{Dl \to Al'} = k_{Dl \to Al} \delta_{ll'}$ ($\delta_{ll'}$ is the Kronecker symbol) and thus the general form of the rate $K_{\mathrm{conc}}^{(\mathrm{f})}$ reads as follows:

$$K_{\rm conc}^{\rm (f)}=k_{DA}=\sum_l Q_l^{(D)}k_{Dl\to Al}. \tag{56}$$

The summation covers all substates ($l=a,b,c,d$). Among the substates related to the initial electronic state D the largest statistical weight belongs to the substates a and c. This is due to the fact that both are characterized by the uptake of a proton near the doubly reduced donor center. Therefore, Eq. (56) can be specified as ($K_{\rm conc}^{(Dl)}\equiv k_{Dl\to Al}$)

$$K_{\rm conc}^{\rm (f)}\simeq f_{\rm p\,D}^{(D)}f_{\rm p\,A}^{(D)}K_{\rm conc}^{(Da)}+f_{\rm p\,D}^{(D)}f_{\rm dp\,A}^{(D)}K_{\rm conc}^{(Dc)}. \tag{57}$$

In accordance with Eq. (41) there exist two limiting cases for the stepwise rates, namely $K_{\rm step}^{\rm (f)}\approx k_{DI}$ if $k_{IA}\gg k_{ID}$ and $K_{\rm step}^{\rm (f)}\approx(k_{DI}/k_{ID})k_{IA}$ if $k_{IA}\ll k_{ID}$. The first limiting case results in an expression for the stepwise transfer rate that depends on the actual pH value in a manner which is identical to the above mentioned dependence of the concerted transfer rate, Eq. (57). The other limiting case is of much more interest. Bearing in mind relation (A10) we may derive

$$K_{\rm step}^{\rm (f)}\approx\frac{Z_I}{Z_D}\sum_l\sum_{l'}Q_l^{(I)}k_{Il\to Al'}. \tag{58}$$

It is not difficult to show that in the case of four protonated-deprotonated substates as displayed in Fig. 6 the ratio of the electronic partition functions reads

$$\frac{Z_I}{Z_D}=(f_{\rm p\,D}^{(D)}f_{\rm p\,A}^{(D)}/f_{\rm p\,D}^{(I)}f_{\rm p\,A}^{(I)})e^{-\Delta G_{ID}/RT}, \tag{59}$$

where ΔG_{ID} is the difference between the free energies of the completely protonated I and D states. Substituting the ratio (59) into Eq. (58), employing the definition (54), and keeping only two main terms (related to substates a and c) one derives

$$K_{\rm step}^{\rm (f)}\approx f_{\rm p\,D}^{(D)}f_{\rm p\,A}^{(D)}K_{\rm step}^{(Ia)}+(f_{\rm p\,D}^{(D)}f_{\rm p\,A}^{(D)}f_{\rm dp\,A}^{(I)}/f_{\rm p\,A}^{(I)})K_{\rm step}^{(Ic)}. \tag{60}$$

Here, each rate constant $K_{\rm step}^{(Il)}\equiv\Sigma_{l'}k_{Il\to Al'}$ includes alternative channels to reach the final electronic state from the concrete substate Il. For instance, the channel $Ia\to Aa$ corresponds to a pure single-electron transfer while the channel $Ia\to Ab$ results in a single-electron transfer accompanied by the removal of the proton from the D center.

Comparsion of Eqs. (57) and (60) shows that the concerted pathway related to the ath substates exceeds the corresponding stepwise pathway only if $K_{\rm conc}^{(Da)}\gg K_{\rm step}^{(Ia)}$. But, in the case of the cth substates it occurs if $K_{\rm conc}^{(Dc)}\gg K_{\rm step}^{(Ic)}(f_{\rm p\,A}^{(D)}f_{\rm dp\,A}^{(I)}/(f_{\rm dp\,A}^{(D)}f_{\rm p\,A}^{(I)})$. If one takes into account Eq. (55) it yields

$$K_{\rm conc}^{(Dc)}\gg K_{\rm step}^{(Ic)}(K_{\rm A}^{(I)}/K_{\rm A}^{(D)}). \tag{61}$$

Since a proton uptake by a center is much more effective when the center has a higher negative charge we may realize that

$$pK_{\rm D}^{(D)}>pK_{\rm D}^{(I)}>pK_{\rm D}^{(A)},\quad pK_{\rm A}^{(D)}<pK_{\rm A}^{(I)}<pK_{\rm A}^{(A)}. \tag{62}$$

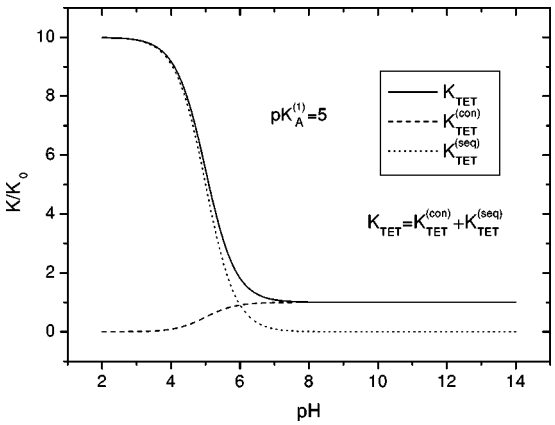

FIG. 7. Example for the replacement of the stepwise pathway by the concerted one. The calculations are based on Eq. (63) with $K_s=10K_0$, $K_c=K_0$.

The inequalities (62) show that due to different values of the parameters $pK_{\rm D}^{(m)}$ and $pK_{\rm A}^{(m)}$ an effective switching of the TET pathways is possible via an alteration of the pH value. This result can be underlined by noting that along with the inequalities (62) the condition $pK_{\rm D}^{(D)}>pK_{\rm A}^{(D)}$ is also valid. Therefore, if one evaluates the pH dependence of the rate constants in the vicinity of $pK_{\rm A}^{(D)}$, the approximation $f_{\rm p\,D}^{(D)}\simeq 1$ can be used since it is fulfilled in an excellent manner. Correspondingly, one obtains

$$K_{\rm TET}^{\rm (f)}=K_{\rm step}^{\rm (f)}+K_{\rm conc}^{\rm (f)},$$

$$K_{\rm step}^{\rm (f)}=\frac{K_s}{1+10^{\,p{\rm H}-p{\rm K}_{\rm A}^{(D)}}},\quad K_{\rm conc}^{\rm (f)}=\frac{K_c}{1+10^{\,pK_{\rm A}^{(D)}-p{\rm H}}}, \tag{63}$$

where K_s and K_c are pH-independent constants characterizing the transfer rates along the sequential and the concerted pathways. Figure 7 shows the switching of the TET pathways caused by the change of the pH value in the vicinity of a certain value of $pK_{\rm A}^{(D)}$. It is clearly seen that the stepwise and the concerted mechanism dominate in two different pH domains.

The scheme of the proton-assisted D-A TET reaction as given in Fig. 6 indicates that the interpretation of the results essentially depends on the weights of the corresponding substates. If the major weights are related to identical substates, e.g., Dc and Ac, the transfer of electrons can be characterized as a pure D-A TET reaction. If the weights Dc and Ab dominate in the respective electronic states D and A, then the D-A TET is accompanied by proton release and proton uptake, and consequently a hydride transfer reaction proceeds. Below we will apply the coarse-grained approach to the description of the transfer of reducing equivalents in mycothione reductase.

IV. TET REDUCTION OF MYCOTHIONE REDUCTASE BY NADPH

Micothione reductase (MycR) catalyzes the nicotinamide adenine dinucleotide phosphate (NADPH)–dependent reduc-

tion of mycothione disulfide. The reduction proceeds as the transfer of two electrons from NADPH to the active-site cysteines, Cys_{44}—S—S—Cys_{39} across the bound FAD (flavin adenine dinucleotide). The catalysis includes a lot of different electron and proton coupled steps. We restrict ourself to the consideration of the two-electron reduction of the enzyme MycR. Detailed experimental studies of this (and other) catalytic steps are reported in Ref. [15] where a minimal kinetic model has been introduced and where an explanation has been given of the chemical mechanism related to the ET events. In particular it has been found that the enzyme reduction by NADPH occurs via single-exponential kinetics with an overall TET rate $K_{\mathrm{red}} \approx 130\ \mathrm{s}^{-1}$. The reduction is fixed by the appearance of the thiol-flavin charge-transfer complex FAD–$(E_{red}H)^-$ with a characteristic absorbance at about 530 nm. (Here and below the symbols E_{ox} and E_{red} stand for the oxidized and the twofold reduced forms, respectively of the enzyme.) A detailed analysis of the *p*H dependence of this reaction given in Ref. [15] shows that, (a) there exists a group X (probably Arg) whose deprotonation at high *p*H values affects the binding of NADPH to MycR, (b) Cys_{44}—S—S—Cys_{39} disulfide is cleaved to generate the dithiolate while Cys_{44} remains ionized (just such an ionization is responsible for the strong charge-transfer interaction with FAD), (c) the protonation of Cys_{39} might slow down the rate of the enzyme reduction, and (d) the very fast step of the common TET process refers to the creation of a FAD–E_{ox}-NADPH charge-transfer complex.

To understand the possible electron-proton transfer pathways in a given TET reaction we consider the transition scheme depicted in Fig. 8. The boxes *A*, *B*, *C*, *D*, and *D′* represent the different electronic states, with box *D′* as the final reduced state which corresponds to the removal of $NADP^+$ from the enzyme. Wavy arrows indicate the fast protonation/deprotonation processes in each electronic state (compare the schemes in Figs. 8 and 6). Note that the following abbreviations have been used in the scheme (R is the His_{444}—H$\cdots$$Glu_{448}$ pair):

$$\mathrm{E_{ox}} = \mathrm{X, Cys_{44}—S—S—Cys_{39}, \ldots, R},$$

$$\mathrm{E_{ox}H} = \mathrm{X, Cys_{44}—S^+,\ \ Cys_{39}—SH, \ldots, R},$$

$$\mathrm{E^-} = \mathrm{X, Cys_{44}—S^-,\ \ S—Cys_{39}, \ldots, R},$$

$$\mathrm{EH} = \mathrm{X, Cys_{44}—S,\ \ Cys_{39}—SH, \ldots, R},$$

$$\mathrm{E_{red}} = \mathrm{X, Cys_{44}—S^-, Cys_{39}—S^-, \ldots, R},$$

$$(\mathrm{E_{red}H})^- = \mathrm{X, Cys_{44}—S^-, Cys_{39}—SH \ldots, R}. \qquad (64)$$

Remember that the coarse-grained description used in the present paper supposes that the TET proceeds against the background of fast protonation/deprotonation processes. Therefore and with noting that the binding of NADPH is also a fast kinetic process the set of kinetic equations looks similar to that of Eq. (A8). This set includes the corresponding transfer rates k_{mn} and describes the evolution of the integral population $P_m(t)$ of each electronic state $m = A,B,C,D,D'$. Note that besides the rates of sequential transfer which are shown in the scheme, there also exists rates k_{BD} and k_{DB} (not shown in the scheme) which characterize the concerted transfer of two electrons. All transfer rates k_{mn} can be evaluated in line with Eq. (A9). For instance, one obtains $k_{BC} = \Sigma_{l_B} \Sigma_{l_C} Q_{l_B}^{(B)} k_{Bl_B Cl_C}$ where the quantity $Q_{l_B}^{(B)} = Z_B^{-1} \exp(-G_{l_B}^{(B)}/RT)$ denotes the weight of the l_Bth substate in the electronic state *B* ($G_{l_B}^{(B)}$ is the free energy of substate l_B in electronic state *B*). To proceed we take into consideration the fact that the FAD reduction takes place on a shorter time scale than the TET between $FADH^-$ and the site Cys_{44}—S—S—Cys_{39}. It means that the TET occurs against the background of much faster transition processes between the *A* and the *B* electronic states. Therefore a quasiequilibrium exists between the populations of both states, i.e., $P_A(t)/P_B(t) = Z_A/Z_B$ [cf. Eq. (A10)]. This circumstance allows us to operate with the integral population $P_1(t) \equiv P_A(t) + P_B(t)$, and we are able to utilize a coarse-grained relation $P_{A(B)}(t) = [Z_{A(B)}/(Z_A + Z_B)] P_1(t)$. Moreover, it is necessary to underline that $NADP^+$ is removed from the

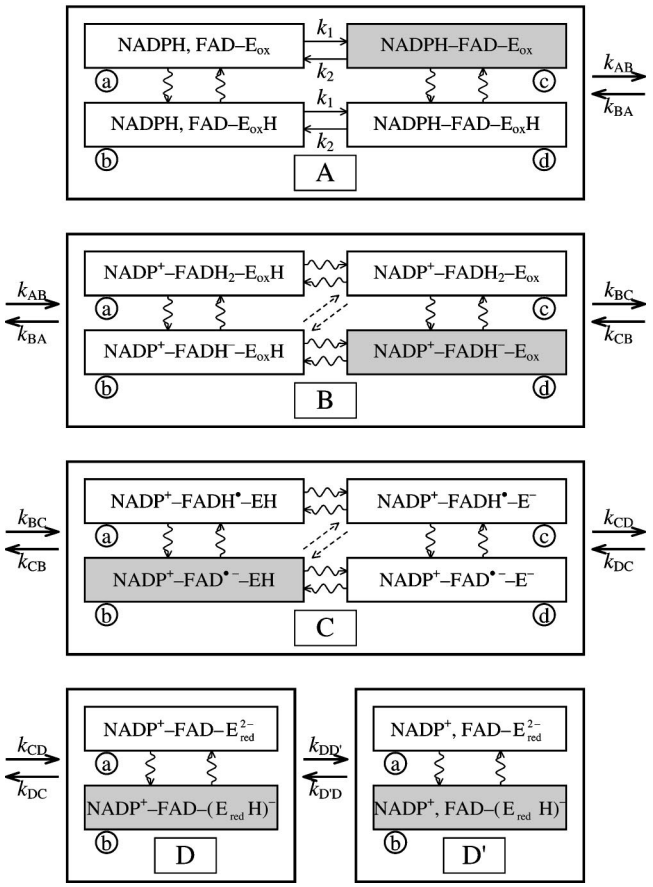

FIG. 8. Scheme for the extended version of proton-assisted two-electron reduction of mycothione reductase. The notation of the enzyme groups which participate in the TET is explained in Eq. (64). Wavy lines indicate the protonation/deprotonation processes. The large boxes represent the electronic states which contain those substates with various groups which accept or release protons (inner boxes). The shaded inner boxes denote the major substates which participate in the formation of the sequential TET pathway.

enzyme rather fast compared to the TET reduction of the enzyme. Therefore, a coarse-grained relation $P_{D(D')}(t) = [Z_{D(D')}/(Z_D+Z_{D'})]P_3(t)$ is also valid and we can introduce an integral population of the final D and D' electronic states, $P_3(t) \equiv P_D(t)+P_{D'}(t)$. The introduction of two integral populations $P_1(t)$ and $P_2(t)$ allows us to operate with a set of three coupled equations

$$\dot{P}_1(t) = -(r+q)P_1(t)+gP_2(t), \tag{65}$$

$$\dot{P}_2(t) = -(g+\kappa)P_2(t)+rP_1(t),$$

$$\dot{P}_3(t) = qP_1(t)+\kappa P_2(t),$$

where the population of the transient electronic state C is denoted by $P_2(t) \equiv P_C(t)$. To derive Eqs. (65), we took into consideration the fact that the quantum yield of the reduced fraction $(E_{red}H)^-$, cf. Eq. (64), is near unity and thus backward rates k_{DC} and k_{DB} are negligible compared with the corresponding forward rates k_{CD} and k_{BD}, respectively. The transfer rates which enter Eqs. (65) are given by

$$r \equiv k_{12} = \frac{Z_B}{Z_A+Z_B} \sum_{l_B} \sum_{l_C} Q_{l_B}^{(B)} k_{Bl_B Cl_C},$$

$$g \equiv k_{21} = \sum_{l_C} \sum_{l_D} Q_{l_C}^{(C)} k_{Cl_C Bl_B},$$

$$q \equiv k_{13} = \frac{Z_B}{Z_A+Z_B} \sum_{l_B} \sum_{l_D} Q_{l_B}^{(B)} k_{Bl_B Dl_D},$$

$$\kappa \equiv k_{23} = \sum_{l_C} \sum_{l_D} Q_{l_C}^{(C)} k_{Cl_C Dl_D}. \tag{66}$$

The exact solution of Eqs. (65) results in two-exponential kinetics. Since the experiment shows a single-exponential behavior we have to suppose that only a minor population of the transient state C is realized in the course of the TET. This means that one has to put $g, \kappa \gg r, q$ which allows us to introduce the following approximate solution:

$$P_D(t) \simeq \left(1 - P_{I\max}\frac{q}{r} - P_{I\max}^2\frac{\kappa}{r}\right)e^{-K_{\mathrm{TET}}t},$$

$$P_I(t) \simeq P_{I\max}e^{-K_{\mathrm{TET}}t},$$

$$P_A(t) \simeq 1 - \left(1 - P_{I\max}\frac{q}{r} + P_{I\max}^2\frac{g}{r}\right)e^{-K_{\mathrm{TET}}t}. \tag{67}$$

Here, $P_{I\max} \simeq r/(\kappa+g)$ is the maximal population of the transient electronic state and

$$K_{TET} = K_{\mathrm{red}} = K_{\mathrm{conc}} + K_{\mathrm{step}} \quad (K_{\mathrm{conc}} = q, \ K_{\mathrm{step}} = P_{I\max}\kappa) \tag{68}$$

denotes the overall transfer rate of the enzyme reduction. The rate (68) contains a contribution from the concerted and a contribution from the stepwise TET mechanism. In the following, we will analyze the pH dependence of both contributions.

In accordance with the experimental findings noted above, there has to exist a certain group X (probably Arg) which, if being in the protonated state, favors the binding of NADPH to the enzyme. Based on the partial statistical sum $\exp(-G_{\mathrm{p}}^{(X)}/RT)+\exp[-(G_{\mathrm{dp}}^{(X)}+RT[H^+])/RT] = \exp(-G_{\mathrm{p}}^{(X)}/RT)[f_{\mathrm{p}}^{(X)}]^{-1}$ which includes the protonated and the deprotonated substates of the X group in the electronic ground state 0 (with the corresponding free energies $G_{\mathrm{p}}^{(X)}$ and $G_{\mathrm{dp}}^{(X)}$), one can introduce a partition function for each electronic state $m = A, B, C, D, D'$ as

$$Z_m = \overline{Z}_m[f_{\mathrm{p}}^{(X)}]^{-1}, \quad \overline{Z}_m = \sum_{l_m} \exp(-G_{l_m}^{(m)}/RT), \tag{69}$$

where $f_{\mathrm{p}}^{(X)} \equiv f_{\mathrm{p\,X}}^{(0)}$ is defined according to Eq. (55), and $G_{l_m}^{(m)}$ is the free energy of the l_mth substate with a protonated X group.

To derive a common pH dependence of the TET transfer rates a precise specification of those major substates which form the electron pathways and which are completely connected with the electronic states B, C, and D becomes necessary. To compare our theoretical model with experimental data we restrict ourself to the consideration of the pH domain from 6 to 10. At such pH values, the weight of the fraction $FADH_2$ in the electronic state B is smaller than the weight of the corresponding fraction $FADH^-$. Besides, it is well known (cf., e.g., [45]) that $FADH^-$ is oxidated in a much more effective way than $FADH_2$. Therefore, the substates b and d in the electronic state B seem to be more likely to participate in TET reaction as the remaining substates a and c. Experimental data on flavin reduction and its reoxidation by disulfide show [46] that the most efficient oxidation of the $FADH^-$ occurs for the disulfide group whether this group is cleaved or protonated. Therefore, in the electronic state B, just the substate d is the major candidate to form the electronic pathways. In contrast, the free energies of all substates of the electronic state A are positioned below the substate energies which belong to the electronic states B and C. As a result of this, one can put $Z_A+Z_B \approx Z_A = \overline{Z}_A[f_{\mathrm{p}}^X]^{-1}$ when calculating the transfer rates given in Eq. (66). To derive a concrete expression for $\overline{Z}_A$ we have to note that the symbols c and d in box A (cf. Fig. 8) indicate the substates with the absorbed NADPH while the symbols b and d refer to the protonated Cys_{39} in the structure Cys_{44}—S—S—Cys_{39}. Denoting by $G_d^{(A)}$ the free energy of substate d which contains the bound NADPH and the protonated Cys_{39}, one derives

$$\overline{Z}_A = \exp(-G_d^{(A)}/RT)[f_{\mathrm{NADPH}}^{(A)} f_{\mathrm{p}}^{(\mathrm{Cys})}]^{-1}. \tag{70}$$

The distribution function $f_{\mathrm{p}}^{(\mathrm{Cys})} \equiv f_{\mathrm{p\,Cys}}^{(A)}$ characterizes the protonation of Cys_{39}. Its concrete expression is given in Eq. (55), where $K_{\mathrm{Cys}}^{(A)} \equiv \exp[-(G_{\mathrm{dp\,Cys}}^{(A)} - G_{\mathrm{p\,Cys}}^{A})/RT]$. Moreover, we have introduced the quantity $f_{[\mathrm{NADPH}]}^{(A)}$

$=[\mathrm{NADPH}]/([\mathrm{NADPH}]+K_{dis})$, which defines the weight of the NADPH-bound fraction of the S-E complex (K_{dis} and [NADPH] are the dissociation constant and the NADPH concentration, respectively).

Formation of the concerted pathway. In line with Eqs. (66) and (68) the concerted transfer rate is expressed via the partial rate constants $k_{Bl_B Dl_D}$. Since, Bd is the dominant substate for the electronic pathways one can write

$$K_{\mathrm{conc}} \simeq \exp(-G_d^{(B)}/RT) Z_A^{-1} \sum_{l_D} k_{Bd \to Dl_D}, \tag{71}$$

where the relation $Z_A + Z_B \approx Z_A$ has been also used. To specify the exponential prefactor we note that the substates Bd and Ad refer to the deprotonated and the protonated group of Cys_{39}, respectively, and to the case where the enzyme exists in the oxidized form [cf. the notation in Eq. (64) and Fig. 8]. Therefore, we set $\exp(-G_d^{(B)}/RT)/Z_A = \exp(-\Delta G_d^{(BA)}/RT)/f_{\mathrm{dp}}^{(\mathrm{Cys})}$, where the quantity $\Delta G_d^{(AB)}$ defines the difference of free energies related to substates Bd and Ad. Note that due to the fact that both electronic states A and B contain the same structures $\mathrm{E_{ox}}$ and $\mathrm{E_{ox}H}$, we have to put $K_{\mathrm{Cys}}^{(A)} \approx K_{\mathrm{Cys}}^{(B)}$. Thus, the function $f_{\mathrm{dp}}^{(\mathrm{Cys})}$ specifies the weight of the substates with the deprotonated group Cys_{39}, i.e., the weight of the fraction $\mathrm{E_{ox}}$ in both electronic states, A and B. Now, the concerted part of the overall transfer rate K_{TET} can be written as

$$K_{\mathrm{conc}} = f_{\mathrm{p}}^{(X)} f_{\mathrm{dp}}^{(\mathrm{Cys})} K_{\mathrm{conc}}^{(0)}. \tag{72}$$

This expression shows that the pH dependence of the concerted transfer rate is completely included in the weights $f_{\mathrm{p}}^{(X)}$ and $f_{\mathrm{dp}}^{(\mathrm{Cys})}$ defined by Eq. (55), while the part

$$K_{\mathrm{conc}}^{(0)} = f_{\mathrm{NADPH}}^{(A)} \exp(-\Delta G_d^{(BA)}/RT) \frac{2\pi}{\hbar} \times \sum_{l_D} |V_{Dl_D Bd}|^2 (FC)_{Bd \to Dl_D} \tag{73}$$

is a pH-independent factor. Just this factor defines the maximal value of the concerted TET rate. It remains to specify the electronic couplings $V_{Dl_D Bd}$ for the TET process.

A direct determination of $V_{Dl_D Bd}$ can be achieved by quantum chemical computations as it has been done to a large extent for single-electron transfer processes [7]. Here, we will remain on a qualitative level and explain one possible mechanism for the formation of the two-electron coupling $V_{Dl_D Bd}$. To this end, one has to note that D-A TET in MycR occurs between the $\mathrm{FADH^-}$ (donor site) and $\mathrm{Cys_{44}—S—S—Cys_{39}}$ (acceptor site), and thus appears as a distant TET. Therefore, a two-electron coupling could be formed via a repeated mechanism of superexchange if one supposes that in line with the scheme of Fig. 8 the transient (intermediate) state is given by the state C while the states B and D act as the donor and acceptor, respectively. In the system under consideration, there exist several single-electron pathways between the donor and the acceptor sites, and thus there must exist several single-electron superexchange couplings responsible for the transitions $B \to C$ (couplings $V_{Ca\,Bb}, V_{Cc\,Bd}$) and for the transitions $C \to D$ (couplings $V_{Db\,Cb}, V_{Da\,Cd}$). Besides, a lot of single-electron pathways are accompanied by the removal or the uptake of a proton. As an example we refer to $V_{Cb\,Bd}$ and $V_{Db\,Cc}$, which are responsible for the mentioned transitions $B \to C$ and $C \to D$, respectively. Experimental results, however, indicate a small population of state C (including all substates l_C). Therefore, in noting Eq. (B4) one derives

$$|V_{Dl_D Bd}|^2 = \frac{|V_{Dl_D Cl_C}|^2 |V_{Cl_C Bd}|^2}{\Delta E_{Cl_C Bd} \Delta E_{Cl_C Dl_D}}. \tag{74}$$

The matrix elements $V_{Cl_C Bd}$ and $V_{Dl_D Cl_C}$ which determine the two-electron coupling $V_{Dl_D Bd}$ are maximal if the corresponding substates Cl_C and Dl_D show a minimal conformational difference with respect to the substate Bd, and if the substates forming the two-electron pathway involve a minimal number of protons (to reduce the number of overlap integrals). In the case under consideration, we derive an expression for $V_{Dl_D Bd}$ by only using pure single-electron couplings (such as $V_{Cb\,Bd}$) and the couplings describing combined electron-proton transitions (such as the coupling $V_{Cc\,Bd}$). Therefore, a two-electron superexchange matrix element $V_{Dl_D\,Bd}$ is formed by two pairs of possible pathways, either with the participation of the virtual Cc or by the participation of the virtual Cb substates. The first pair corresponds to the channels $Bd \to Cc \to Da$ and $Bd \to Cc \to Db$, while the second pair of pathways is associated with the channels $Bd \to Cb \to Da$ and $Bd \to Cb \to Db$. Each of the channels contains the pure electron transition and the proton-assisted electron transition. As an example we refer to the channel $Bd \to Cc \to Db$, where the $(Bd \to Cc)$ and the $(Cc \to Db)$ pathways refer to pure single-electron and proton-assisted electron transitions, respectively. Another example is given by the channel $Bd \to Cb \to Db$, where the pathway $Bd \to Cb$ is associated with a single-electron transfer accompanied by the proton displacement within the enzyme, while pathway $Cb \to Db$ refers to a pure single-electron transfer.

Formation of the stepwise pathway. It has been already mentioned that the representation of the overall transfer rate by adding contributions from the concerted and stepwise mechanisms of TET, Eq. (68), is correct at a rather small population of the transient state ($P_{I\max} < 10^{-2}$). Just in this case the substates Cl_C can be considered as virtual intermediate substates which are responsible for the formation of a two-electron superexchange coupling between the initial and the final states denoted in Fig. 8 by B and D, respectively. The principal difference between the stepwise mechanism and the concerted one is related to the fact that within the stepwise donor-acceptor TET the transition state C acts as a state which really becomes populated although its total population remains small. It means that the stepwise pathway appears as a hopping process of electrons between the substates belonging to the electronic states B, C, and D. The concrete form of the stepwise transfer rate $K_{\mathrm{seq}} = r\kappa/(g+\kappa)$ follows

from Eq. (68). As far as the electronic states C and B are intermediates for the initial state A and the final state D (including D') we can suppose that $k_{CB} \gg k_{CD}$, i.e., $g \gg \kappa$. This yields $K_{\rm seq} \approx (Z_C/Z_A)\kappa$, where the relation $r/g = k_{12}/k_{21} = Z_C/(Z_A+Z_B) \approx Z_C/Z_A$ has been used. The main contribution to the transfer rate $\kappa = k_{23}$ follows from the channels which are associated with the oxidation of $FADH^{\cdot -}$ rather than of $FADH^-$. This fact is supported by the data on electron/proton transfer in flavoproteins [45]. Therefore, the substates b and d of the transient state C are preferable candidates to participate in the stepwise pathway. Note now that in contrast to the electronic state B where the enzyme MycR is not reduced yet, the state C corresponds to a singly reduced enzyme. The location of the transferred electron within the enzyme is associated with one of the Cys residue [for the definition of E^- and EH see Eq. (64)]. Therefore, for the pH range of 6–10 under consideration the appearance of an extra negative charge on sulfur makes the substate EH where a proton has been absorbed more stable than the ionized state E^- of the enzyme.

Of even greater importance is the fact that in the final electronic state D just the substate Db with the proton coupled to Cys_{39} specifies a stable dithiolate while Cys_{44} remains ionized and creates the charge-transfer complex $FAD-(E_{red}H)^-$, Eq. (64). Therefore, the most effective hopping channel which lets one move an electron from state C to state D can be associated with the transition $Cb \to Db$. This yields $\kappa \approx k_{CD} = Q_b^{(C)} k_{Cb\,Db}$. Note that the given one-particle hop corresponds to a pure electron transfer and thus has to be thought of to be more effective than the, e.g., more complicated electron hops $Cb \to Da$ or $Cd \to Db$, where the ET is accompanied either by a proton removal or by a proton uptake, respectively. (In Fig. 8 the most important substates forming the stepwise pathway are indicated by the inner shaded boxes.) The final form of the stepwise forward TET rate follows from the expression $K_{\rm step} \approx \exp(-G_b^{(C)}/k_BT) Z_A^{-1} k_{Cb\,Db}$. Introducing the pH-independent factor $K_{\rm step}^{(0)}$ the stepwise transfer rate of the two-electron enzyme reduction reaction can be represented as

$$K_{\rm step} = f_{\rm p}^{(X)} K_{\rm step}^{(0)}, \tag{75}$$

with the pH-independent factor

$$K_{\rm step}^{(0)} = f_{\rm NADPH}^{(A)} \exp(-\Delta G_d^{(CA)}/RT) \frac{2\pi}{\hbar} |V_{Db\,Cb}|^2 (FC)_{Cb \to Db}. \tag{76}$$

In line with Eq. (55) the function $f_{\rm p}^{(X)}$ decreases with the decrease of proton concentration $[H^+]$. Therefore, the stepwise transfer rate (75) decreases only when the pH increases. In contrast, the function $f_{\rm dp}^{(\rm Cys)}$ increases with increasing pH. As a result we obtain a bell-shaped pH-dependence of the concerted transfer rate (72) which is defined by the product of $f_{\rm p}^{(X)}$ and of $f_{\rm dp}^{(\rm Cys)}$. Hence, it becomes obvious that the concerted and the stepwise contribution are characterized by a different pH dependence.

Figure 9 shows the pH-dependence of the two-electron MycR reduction. The experimental data are best fitted

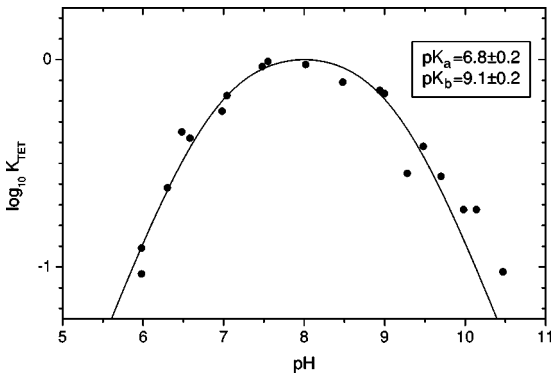

FIG. 9. pH dependence of the two-electron reduction reaction of mycothione reductase. The points correspond to the experimental data of Ref. [15]. The theoretical curve follows from the concerted mechanism of proton-assisted TET, Eq. (72).

to the pH-dependence $\log_{10} y = \log_{10}\{C/(1+[H^+]/K_a + K_b/[H^+])\}$ in using $pK_a = 6.8 \pm 0.2$ and $pK_b = 9.1 \pm 0.2$ [15]. The groups exhibiting pK values of 6.8 ± 0.2 and 9.1 ± 0.2 are Cys and presumably Arg, respectively. Protonation and deprotonation of the corresponding groups decreases the TET reduction of the enzyme MycR (see the detailed discussion in Ref. [15]). Utilizing $pK^{(\rm Cys)} = 6.8$ and $pK^{(\rm X)} = 9.1$ we see that the theoretical curve $K_{\rm TET} = K_{\rm TET}(p{\rm H})$, Eq. (72) describes the measured pH dependence with a rather good accuracy. Therefore, just the concerted mechanism of TET probably should dominate the reactions and thus should be used to explain the experiments.

V. CONCLUSION

In the present paper we have considered different types of concerted and stepwise pathways controlling bridge-mediated two-electron transfer (TET) reactions. It has been shown that at small bridge populations (less than 10^{-2}) the complex multiexponential TET process can be reduced to a simple two-exponential electron transfer process between three distinct two-electron states, the initial (donor) state $D \equiv D^{2-}BA$ with both electrons at the donor, the intermediate/transient state $I \equiv D^-BA^-$, and the state $A \equiv DBA^{2-}$ with both electrons at the acceptor. If, additionally, the population of the intermediate electronic state remains small (less than 10^{-2}) the TET is reduced to a single-exponential process, Eq. (39), i.e., reduced to a D-A TET reaction. In this case, the corresponding overall transfer rate, Eq. (40), contains an additive contribution from the stepwise and the concerted pathways. The stepwise pathway is originated by sequential and superexchange single-electron transfer processes which differ in their dependence on the bridge length. In contrast, the concerted pathway is a specific two-electron superexchange process based on repeated single-electron superexchange through the bridging states (3) and (5) as well as through the intermediate state (4).

Special attention has been put on the pH dependence of the reaction. Therefore, D-A TET has been studied for those cases where it is accompanied by a fast uptake and/or release

of protons which becomes possible if the protonated structure groups carry out a proton exchange with the surrounding solvent. As far as the protonation/deprotonation process is faster than the nonadiabatic TET, the weights of the protonated and the deprotonated substates, Eq. (54), determine the probability for each ET channel participating in the concerted or the stepwise pathway. The different pH dependence of the concerted and the stepwise contribution to the overall D-A TET rate just results from the presence of this transient state. According to this state the protonated and deprotonated substates contribute differently to the formation of the particular electronic pathways. The proposed model shows that the participation of protonated and deprotonated substates in the initial, transient, and final electronic state reduces the proton-assisted TET to three types of D-A TET: (i) the completely electronic D-A TET, (ii) the hydride D-A TET, and (iii) the two-proton involved D-A TET. Which type of TET reaction takes place is fixed by the weights of the most important substates participating in the TET. This fact could be demonstrated by a comparison of the theoretical model with available experimental data on the TET reduction of micothione reductase by NADPH. Our analysis of the possible electronic pathways indicates that the TET-reduction process of the enzyme can proceed through the concerted mechanism of proton-assisted TET. Just in this case the computed pH dependence of the TET reduction reproduces the measured data rather well. We have also discussed a possible mechanism of the formation of distant two-electron superexchange coupling, Eq. (74), between the $FADH^-$ (donor site) and Cys_{44}—S—S—Cys_{39} (acceptor site) via virtual substates of the transient electronic state C. The concrete form of the coupling is shown to express the product of single-electron superexchange couplings between the substates belonging either to the B and C or to the C and D electronic states (cf. notations in scheme in Fig. 8). Thus the discussed mechanism of the formation of a TET superexchange process between the initial donor and final acceptor states can be described by a repeated single-electron superexchange through the intermediate virtual electronic state C.

Finishing the discussion we note that the derived expressions for the sequential and superexchange transfer rates, Eqs. (47) and (53), respectively, follow from the model of a regular bridge where only the couplings between the terminal bridge groups and the adjacent donor and acceptor centers depend on the charging of these centers. The interior bridge energies and the intersite bridge couplings have been assumed to be independent of the distance from the D and the A sites. Such a phenomenological model serves as the basis for the investigation of numerous transfer processes in molecular systems (see, for instance, Refs. [3,5–8]). In the framework of such a model the bridge-length dependence of the sequential and the superexchange contribution is determined by different decay parameters (43)–(46). Recently, this model has been successfully applied to the explanation of experimental data on single-electron D-A transfer through proline chains [42]. Generally, if studying the length dependence of rate constants, one has to carefully account for the influance of the Coulomb interections between the charges. Just this interaction is able to destroy the regularity of the bridge through the dependence of the local energy levels and reorganization energies on the position of the transferred electrons within the DBA system (see, for example, the discussion in Ref. [47]).

ACKNOWLEDGMENTS

The support of this work by the Volkswagen-Stiftung, Germany, priority area *Intramolecular and Intermolecular Electron Transfer* is gratefully acknowledged.

APPENDIX A: KINETIC EQUATIONS FOR THE DESCRIPTION OF NONADIABATIC BRIDGE-MEDIATED TET PROCESSES

If an electron transfer proceeds against the background of fast vibrational relaxation, one can employ a coarse-grained approach [40,41] to derive kinetic equations for the integral site populations $P_m(t)$. In the case under consideration an electronic state m is characterized by N_m substates denoted by l_m. In order to derive kinetic equations for the populations $P_M(t)$ $(M \equiv ml_m)$ we follow Refs. [40,41]. The approach starts with the Hamiltonians (12) and (13) and leads to the following set of kinetic equations:

$$\dot{P}_{ml_m}(t) = -\left(\sum_{l'_m \neq l_m}^{N_m} \kappa_{ml_m \to ml'_m} + \sum_{n \neq m} \sum_{l_n=1}^{N_n} k_{ml_m \to nl_n} \right) P_{nl_n}(t) + \sum_{l'_m \neq l_m}^{N_m} \kappa_{ml'_m \to ml_m} P_{ml'_m}(t) + \sum_{n \neq m} \sum_{l_n=1}^{N_n} k_{nl_n \to ml_m} P_{nl_n}(t). \tag{A1}$$

The rate constants

$$k_{ml_m \to nl_n} = \frac{2\pi}{\hbar} |V_{nl_n ml_m}|^2 (FC)_{ml_m \to nl_n} \tag{A2}$$

characterize the transitions between the l_mth and l_nth substates related to different electronic states m and n. According to the nonadiabatic nature of the transitions the rates are given as a product of a pure electronic factor and the Franck-Condon factor, FC. This separation implies the Condon approximation $V_{M\{v_M\}M'\{v'_{M'}\}} \approx \langle \{v_M\} | \{v'_{M'}\} \rangle V_{MM'}$, where $\langle \{v_M\} | \{v'_{M'}\} \rangle$ denotes the overlap integral between the vibrational states while $V_{MM'}$ is the electronic coupling between the electronic substates $M = ml_m$ and $M' = m'l_{m'}$. The concrete form of the Franck-Condon factor is detemined by the used model for the vibrations and their coupling to the elctronic states (cf. Refs. [3,5,7,41,42,48,49]).

In contrast to the foregoing type the rate constants $\kappa_{ml_m \to ml'_m}$ are responsible for transitions between the substates l_m and l'_m belonging to the same mth electronic state. Their form is similar to that given in Eq. (A2), but the interaction matrix elements $V_{nl_n ml_m}$ have to be replaced, $\langle ml'_m | H^{(NA)} | ml_m \rangle$, where $H^{(NA)}$ denotes the electronic nona-

diabatic coupling operator [48,49]. Obviously, the processes which are characterized by the rate constants $\kappa_{ml_m \to ml'_m}$ do not change the spatial position of the transferred electrons within the DBA system in contrast to those processes governed by the intersite rate constants (A2).

The kinetic equations (A1) are valid for a time scale much larger than $\tau_{\rm rel}$ (in molecular systems $\tau_{\rm rel}$ typically amounts to values between 0.1 and 10 ps [50,51]). Since nonadiabatic TET is considered the rates (A2) have to be much smaller than the rates $\kappa_{ml_m \to ml'_m}$. This requires that the TET has to also proceed against the background of fast substate-substate transitions within each electronic state. Therefore, the characteristic time $\tau_{\rm subst}$ of these transitions is much smaller than the time $\tau_{\rm TET}$ of the TET itself [cf. basic inequality (1)]. This inequality allows one to perform an additional coarse-graining reduction of Eq. (A1). To this end we introduce the total population of the mth electronic state:

$$P_m(t) = \sum_{l_m} P_{ml_m}(t). \tag{A3}$$

These quantities are related to particular spatial positions of both transferred electrons within the DBA system [cf. Eqs. (2)–(6)] and fulfil the normalization condition $\Sigma_m P_m(t) = 1$. Next we note that at $t \gg \tau_{\rm subst}$ the substate populations satisfy a quasiequilibrium condition $P_{ml_m}(t)/P_{ml'_m}(t) = Z_{ml_m}/Z_{ml'_m}$ with

$$Z_{ml_m} = \sum_{\{v_{l_m}\}} \exp[-E(ml_m\{v_{l_m}\})/k_B T] \tag{A4}$$

being the partition function of the l_mth electronic state. Then, one may derive

$$P_{ml_m}(t) = Q_{l_m}^{(m)} P_M(t). \tag{A5}$$

To define the statistical weight of substate l_m in the mth electronic state,

$$Q_{l_m}^{(m)} = Z_{ml_m}/Z_m, \tag{A6}$$

one has to calculate the partition function of the mth electronic state

$$Z_m = \sum_{l_m} Z_{ml_m}. \tag{A7}$$

Equation (A5) indicates that at $t \gg \tau_{\rm subst}$ the partial (substate) population changes only via a change of the integral populations of the electronic states. According to Eqs. (A1), (A3), and (A5) these populations satisfy the following set of coarse-grained rate equations:

$$\dot{P}_m(t) = -\sum_{n \neq m} [k_{mn} P_m(t) - k_{nm} P_n(t)], \tag{A8}$$

where the intersite transfer rates read

$$k_{mn} \equiv k_{m \to n} = \sum_{l_m=1}^{N_m} \sum_{l_n=1}^{N_n} Q_{l_m}^{(m)} k_{ml_m \to nl_n}. \tag{A9}$$

These rates satisfy the balance conditions

$$k_{nm}/k_{mn} = Z_m/Z_n, \tag{A10}$$

and accumulate contributions of various ET channels each of which is related to the transfer between the substates l_m and l_n. The efficiency of each channel $l_m \to l_n$ is determined by the statistical weight $Q_{l_m}^{(m)}$ of the reactant substate l_m, Eq. (A6), and the corresponding partial rate constant $\kappa_{ml_m \to nl_n}$, Eq. (A2). Choosing the electronic states m and n as those given by Eqs. (2)–(6) we obtain the Eqs. (14)–(22) where three types of rate constants characterize the TET. (Note that for a regular bridge we have set $\alpha \equiv k_{mm+1}$ and $\beta \equiv k_{m+1\,m}$.)

APPENDIX B: SUPEREXCHANGE AT D-A TET

The coupling matrix elements $V_{nl_n\, ml_m}$ are those quantities which specify the type of rate constants k_{mn} in the TET process [see Eqs. (A2) and (A9)]. Single-electron transitions between nearest-neighbored sites of electron location are defined by a direct overlapping of the corresponding electronic wave functions. Such an overlapping defines the couplings $V_{1l_1 Dl_D}, V_{Nl_N Al_A}$ and $V'_{1l'_1 Dl'_D}, V'_{Nl'_N Al'_A}$ which are related to the first and the second step of the TET process, respectively. Moreover, intersite bridge couplings $V_{Bl_m l'_{m+1}} \equiv V_{ml_m m+1 l'_{m+1}}$ are also defined by electronic overlapping integrals between neighboring units. At the same time the couplings $V_{Dl_D Il_I}$, $V_{Il_I Al_A}$, and $V_{Dl_D Al_A}$ are formed owing to the consecutive overlapping of wave functions of the D, the B, and the A units (superexchange mechanism). It is a specific property of the coarse-grained iteration procedure (see Appendix A and Refs. [40,41]) that it not only allows one to derive the set of rate equations and corresponding rate constants but it also determines the superexchange electronic couplings, $V_{Dl_D Il_I}$, $V_{Il_I Al_A}$, and $V_{Dl_D Al_A}$.

We present the form of these quantities for the case of deep tunneling between the states $|D\rangle$, $|I\rangle$, and $|A\rangle$ (see Eqs. (2), (4) and (6), respectively). In the simplest case where further electronic substates are absent an iteration procedure yields (the indices l_D, l_A, l_{B_m}, and $l_{\tilde{B}_n}$ have been omitted)

$$|V_{DI}|^2 = \frac{|V_{D1} V_B^{N-1} V_{NA}|^2}{(\Delta E_D \Delta E_I^{(1)})^N},$$

$$|V_{IA}|^2 = \frac{|V'_{D1} V_B^{N-1} V'_{NA}|^2}{(\Delta E_A \Delta E_I^{(2)})^N},$$

$$|V_{DA}|^2 = \frac{|V_{D1} V_B^{N-1} V_{NA} V'_{D1} V_B^{N-1} V'_{NA}|^2}{[\Delta E_D \Delta \tilde{E}_D \Delta E_A \Delta \tilde{E}_A]^N \Delta E_{ID} \Delta E_{IA}}. \tag{B1}$$

The different types of energy gaps are given in Fig. 1, and we have additionally introduced the energy differences

$\Delta\tilde{E}_D = E(\mathrm{DB}^-\mathrm{A}^-) - E(\mathrm{D}^{\cdot -}\mathrm{BA})$, $\Delta\tilde{E}_A = E(\mathrm{D}^-\mathrm{B}^-\mathrm{A}) - E(\mathrm{DBA}^{2-})$, $\Delta E_{ID} = E(\mathrm{D}^{2-}\mathrm{BA}^-) - E(\mathrm{D}^{\cdot -}\mathrm{BA}) = \Delta E_D - \Delta E_I^{(1)}$, and $\Delta E_{IA} = E(\mathrm{D}^-\mathrm{B}^-\mathrm{A}) - E(\mathrm{DBA}^{2-}) = \Delta E_A - \Delta E_I^{(2)}$. It follows from the definition of the electronic states that $\Delta\tilde{E}_D = \Delta E_{ID} + \Delta E_I^{(2)}$, $\Delta\tilde{E}_A = \Delta E_{IA} + \Delta E_I^{(1)}$, and thus if $\Delta E_{ID} \ll \Delta E_I^{(2)}$ and $\Delta E_{IA} \ll \Delta E_I^{(1)}$, we may identify

$$|V_{DA}|^2 = \frac{|V_{DI}|^2 |V_{IA}|^2}{\Delta E_{ID} \Delta E_{IA}}. \tag{B2}$$

Since the quantities V_{DI} and V_{IA} refer to single-electron superexchange couplings the formula for $|V_{DA}|^2$ clearly indicates that the two-electron superexchange is originated by repeated single-electron superexchange transitions.

If the electronic states are characterized by additional substates, then the superexchange couplings do not only depend on the substates l_D, l_I, and l_A but also on the bridge substates l_m $(m = B_1, B_2, \ldots, B_N)$ and l'_n $(n = \tilde{B}_1, \tilde{B}_2, \ldots, \tilde{B}_N)$. Here we will only restrict our consideration to the case of a rigid bridge where the electronic states of the bridge units do not split off into various substates. The corresponding single-electron couplings read

$$|V_{Dl_D Il_I}|^2 = \frac{|V_{Dl_D 1} V_B^{N-1} V_{NAl_A}|^2}{(\Delta E_{Dl_D} \Delta E_{Il_I}^{(1)})^N},$$

$$|V_{Il_I Al_A}|^2 = \frac{|V'_{Dl_D 1} V_B^{N-1} V'_{NAl_A}|^2}{(\Delta E_{Al_A} \Delta E_{Il_I}^{(2)})^N}, \tag{B3}$$

where the energy gaps ΔE_{Dl_D}, $\Delta E_{Il_I}^{(1)}$, ΔE_{Al_A}, and $\Delta E_{Il_I}^{(2)}$ are completely analogous to the above mentioned energy gaps ΔE_D, $\Delta E_I^{(1)}$, ΔE_A, and $\Delta E_I^{(2)}$, respectively.

For the two-electron coupling we only present the expression which is valid for $\Delta E_{Il_I Dl_D} \ll \Delta E_{Il_I}^{(2)}$ and $\Delta E_{Il_I Al_A} \ll \Delta E_{Il_I}^{(1)}$ (compare this with the above given inequalities $\Delta E_{ID} \ll \Delta E_I^{(2)}$ and $\Delta E_{IA} \ll \Delta E_I^{(1)}$),

$$|V_{Dl_D Al_A}|^2 = \frac{|V_{Dl_D Il_I}|^2 |V_{Il_I Al_A}|^2}{\Delta E_{Il_I Dl_D} \Delta E_{Il_I Al_A}}. \tag{B4}$$

Here, the $\Delta E_{Il_I Dl_D}$ $(\Delta E_{Il_I Al_A})$ are the energy gaps between the l_Ith intermediate and the l_Dth donor (l_Ath acceptor) two-electron substate.

[1] D. DeVault, *Quantum-Mechanical Tunneling in Biological Systems*, 2nd ed. (Cambridge University Press, London, 1984).
[2] E.G. Petrov, *Physics of Charge Transfer in Biosystems* (Naukowa Dumka, Kiev, 1984) (in Russian).
[3] R.A. Marcus and N. Sutin, Biochim. Biophys. Acta **811**, 265 (1985).
[4] G. Zundel, J. Mol. Struct. **177**, 43 (1988).
[5] B.H. Gray and J.R. Winkler, Annu. Rev. Biochem. **65**, 537 (1996).
[6] O. Farver and I. Pecht, Adv. Chem. Phys. **107**, 555 (1999).
[7] Adv. Chem. Phys. **106** (1999), special issue on electron transfer from molecules to biomolecules, edited by J. Jortner and M. Bixon.
[8] D.N. Beratan, J.N. Onuchic, and H.B. Gray, in *Metal Ions in Biological Systems*, edited by H. Sigel and A. Sigel (Marcel Dekker, New York, 1991), Vol. 27, pp. 97–127.
[9] B.K. Burgess and J.L. Lowe, Chem. Rev. (Washington, D.C.) **96**, 2983 (1996).
[10] P.E.M. Siegbahn and M.R. Blomberg, Chem. Rev. (Washington, D.C.) **100**, 421 (2000).
[11] A. Niemz, J. Imbriglio, and V.M. Rotello, J. Am. Chem. Soc. **119**, 887 (1997).
[12] T.T. Chin, W.E. Geiger, and A.L. Rheingold, J. Am. Chem. Soc. **118**, 5002 (1996).
[13] Z.-R. Zheng and D.H. Evans, J. Am. Chem. Soc. **121**, 2941 (1999).
[14] M.-H. Baik, T. Ziegler, and C.K.J. Schauer, J. Am. Chem. Soc. **122**, 9143 (2000).
[15] A.A. Patel and J.S. Blanchard, Biochemistry **40**, 5119 (2001).
[16] Per E.M. Siegbahn and R.H. Crabtree, J. Am. Chem. Soc. **119**, 3103 (1997).
[17] Per E.M. Siegbahn, Inorg. Chem. **38**, 2880 (1999).
[18] T.C. Brunold and E.I. Solomon, J. Am. Chem. Soc. **121**, 8288 (1999).
[19] L.D. Zusman and D.N. Beratan, J. Chem. Phys. **105**, 165 (1996); J. Phys. Chem. A **101**, 4136 (1997); J. Chem. Phys. **110**, 10 468 (1999).
[20] T. Bandyopadhyay, A. Okada, and M. Tachiya, J. Chem. Phys. **110**, 9630 (1999).
[21] R. Marcus, Annu. Rev. Phys. Chem. **15**, 155 (1964); R. Marcus, Angew. Chem. **105**, 101 (1993).
[22] A. Butler and J.V. Walker, Chem. Rev. (Washington, D.C.) **93**, 1937 (1993).
[23] P.K. Agarwal, S.P. Webb, and S. Hammes-Schiefer, J. Am. Chem. Soc. **122**, 4803 (2000).
[24] I.-S.H. Lee, E.H. Jeoung, and M.M. Kreevoy, J. Am. Chem. Soc. **119**, 2722 (1997).
[25] M. Morillo and R.I.J. Cukier, Chem. Phys. **92**, 4833 (1990).
[26] S. Hammes-Schiffer and J.C. Tully, J. Chem. Phys. **99**, 101 4657 (1994).
[27] D. Borgis and J.T. Hynes, J. Phys. Chem. **100**, 1118 (1996).
[28] R.I. Cukier and J. Zhu, J. Phys. Chem. B **101**, 7180 (1997).
[29] R.I. Cukier and D.G. Nocera, Annu. Rev. Phys. Chem. **49**, 337 (1998).
[30] S. Hammes-Schiffer, Acc. Chem. Res. **34**, 273 (2001).
[31] R.I. Cukier, J. Phys. Chem. B **106**, 1746 (2002).
[32] J.P. Roth, S. Lovell, and J.M. Mayer, J. Am. Chem. Soc. **122**, 5486 (2000).
[33] L.J.C. Jeuken, A.K. Jones, S.K. Chapmen, G. Cecchini, and F.A. Armstrong, J. Am. Chem. Soc. **124**, 5702 (2002).
[34] A. Okada, V. Chernyak, and J. Mukamel, J. Phys. Chem. **102**, 1241 (1998).
[35] A.K. Felts, W.T. Pollard, and R.A. Friesner, J. Phys. Chem. **99**, 2929 (1995).

[36] D. Segal, A. Nitzan, W.B. Davis, M.R. Wasielewski, and M.A. Ratner, J. Phys. Chem. B **104**, 3817 (2000).
[37] D. Segal and A. Nitzan, Chem. Phys. **281**, 235 (2002).
[38] A. Nitzan, Annu. Rev. Phys. Chem. **52**, 681 (2001).
[39] M. Bixon and J. Jortner, Chem. Phys. **281**, 393 (2002).
[40] E.G. Petrov, Ye.V. Shevchenko, V.I. Teslenko, and V. May, J. Chem. Phys. **115**, 7107 (2001).
[41] E.G. Petrov and V. May, J. Phys. Chem. A **105**, 10 176 (2001).
[42] E.G. Petrov, Eu.V. Shevchenko, and V. May, Chem. Phys. **288**, 269 (2003).
[43] E.G. Petrov and V. May, J. Chem. Phys. (to be published).
[44] E.G. Petrov and P. Hänggi, Phys. Rev. Lett. **86**, 2862 (2001); E.G. Petrov, P. Hänggi, and V. May, Chem. Phys. **281**, 211 (2002).
[45] R. Hille and R.F.J. Anderson, Biol. Chem. **276**, 31 193 (2001).
[46] C.H. Williams, Jr., L.D. Arscott, S.M. Müller, B.W. Lennon, M.L. Ludvig, P.-F. Wang, D.M. Veine, K. Becker, and R.H. Schirmer, Eur. J. Biochem. **267**, 6110 (2000).
[47] G.S. Tong, I.V. Kurnikov, and D.N. Beratan, J. Phys. Chem. B **106**, 2381 (2002).
[48] V. May and O. Kühn, *Charge and Energy Transfer Dynamics in Molecular Systems* (Wiley-VCH, Berlin, 1999).
[49] F.K. Fong, *Theory of Molecular Relaxation* (Wiley-Interscience, New York, 1975).
[50] M. Cho and C.R. Fleming, Adv. Chem. Phys. Series **107**, 311 (1999).
[51] W.T. Pollard, A. K Felts, and R.A. Friesner, Adv. Chem. Phys. Series **93**, 77 (1996).